

Learning Data Dependency with Communication Cost

Hyeryung Jang[†], HyungSeok Song[†], and Yung Yi^{†*}

Abstract

In this paper, we consider the problem of recovering a graph that represents the statistical data dependency among nodes for a set of data samples generated by nodes, which provides the basic structure to perform an inference task, such as MAP (maximum a posteriori). This problem is referred to as structure learning. When nodes are spatially separated in different locations, running an inference algorithm requires a non-negligible amount of message passing, incurring some communication cost. We inevitably have the trade-off between the accuracy of structure learning and the cost we need to pay to perform a given message-passing based inference task because the learnt edge structures of data dependency and physical connectivity graph are often highly different. In this paper, we formalize this trade-off in an optimization problem which outputs the data dependency graph that jointly considers learning accuracy and message-passing costs. We focus on a distributed MAP as the target inference task due to its popularity, and consider two different implementations, **ASync-MAP** and **Sync-MAP** that have different message-passing mechanisms and thus different cost structures. In **ASync-MAP**, we propose a polynomial time learning algorithm that is optimal, motivated by the problem of finding a maximum weight spanning tree. In **Sync-MAP**, we first prove that it is NP-hard and propose a greedy heuristic. For both implementations, we then quantify how the probability that the resulting data graphs from those learning algorithms differ from the ideal data graph decays as the number of data samples grows, using the large deviation principle, where the decaying rate is characterized by some topological structures of both original data dependency and physical connectivity graphs as well as the degree of the trade-off, which provides some guideline on how many samples are necessary to obtain a certain learning accuracy. We validate our theoretical findings through extensive simulations, which confirms that it has a good match.

1 Introduction

In many online/offline systems with spatially-separated agents (or nodes), a variety of applications involve distributed in-network statistical inference tasks, which have been

^{*†}: Department of Electrical Engineering, KAIST, South Korea, e-mails: hrjang@lanada.kaist.ac.kr, hssong@lanada.kaist.ac.kr, yiyung@kaist.edu. Address for Correspondence: Yung Yi, KAIST 291, Daehak-ro, Yuseong-gu, Daejeon, 305-701, South Korea.

widely studied, exploiting given knowledge of statistical dependencies among agents. As one example, in sensor networks with multiple targets, each sensor node measures the target-specific information in its coverage area (*e.g.*, position, direction, distance), which further has a correlation among sensors. One well-recognized inference problem is a data association which determines the correct match between measurements of sensors and target tracks by maximum a posteriori (MAP) estimation that is executed in a distributed fashion by exchanging some information messages. Other examples include target tracking, and detection/estimation in sensor networks [1, 2, 3, 4] and de-anonymization, rumor/infection propagation in social networks [5, 6, 7, 8].

To solve these distributed in-network inference problems, it is of crucial importance to understand how data from nodes are inter-dependent. To that end, a notion of the *graphical model* has been one of the powerful frameworks in machine learning for a succinct modeling of the statistical uncertainty, where each node in the graphical models corresponds to a random variable and each edge specifies the statistical dependency between random variables. A wide variety of scalable inference algorithms on graphical models via message-passing have been developed, of which examples include belief propagation (BP) or max-product with a certain degree of convergence and accuracy guarantees [9, 10, 11, 12]. This graphical model, which we also call data dependency graph or simply data graph throughout this paper, is not given a priori, and it should be learnt only by using a given set of data samples from nodes. This problem, referred to as *graph learning* or *structure learning* [13, 14, 15, 16], has been an active research topic in statistical machine learning.

In this paper, for a collection of n data sample vectors generated by nodes, we study a problem of graph learning, which also considers the communication cost incurred by the distributed in-network inference algorithm being applied to the learnt data graph. Physical communication cost often becomes a critical issue, for example, exerting a significant impact on the lifetime of networked sensors. Clearly, there exists a trade-off between the amount of incurred cost and the learning accuracy of the data graph. Figure 1(a) illustrates the physical connection among 7 sensors, which differs from the exact data dependency graph in Figure 1(b). The sensor nodes s_1 and s_6 have non-negligible data dependency, requiring message-passing when performing inference, but they are three hops away from each other, incurring a large amount of communication cost. In this case, one may want to sacrifice the estimation accuracy a little bit and reduce communication cost by utilizing the data graph as shown in Figure 1(c). As done in many prior works on graph learning [16, 17, 18, 19], we restrict our attention to tree-structured data graphs due to its simplicity, yet a large degree of expressive powers and other benefits, *e.g.*, some inference algorithms such as BP over tree-structured data graphs become optimal.

We now summarize our contributions in what follows:

- (a) We first formulate an optimization problem of learning data graph, having as an objective function the weighted sum of learning accuracy and the amount of cost that will be incurred by a distributed inference algorithm. Out of many possible inference algorithms, we consider the maximum a posteriori (MAP) estimator that is popular for many inference tasks, and two versions for the MAP implementation: (i) asynchronous and (ii) synchronous, which we call **ASYNC-MAP** and **SYNC-**

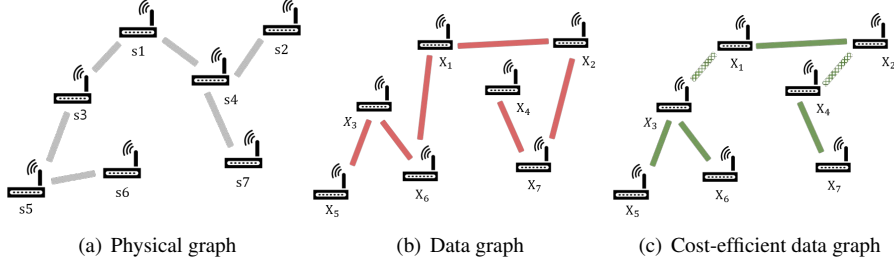


Figure 1: Network graphs with 7 sensors. (a) physical connectivity, (b) exact statistical dependency graph called data graph, (c) Data graph considering communication cost between nodes.

MAP. These implementations have different patterns of passing messages, thus leading to different forms of communication costs, being useful to understand how distributed algorithms’ cost affect the resulting data dependency graph.

- (b) Next, for **ASYNC-MAP** we develop a polynomial-time algorithm to find an optimal (cost-efficient) data graph that corresponds to simply finding a maximum weight spanning tree. This simplicity stems from the cost structure of **ASYNC-MAP** that is characterized only by the sum of all ‘localized’ edge costs. Being in sharp contrast to **ASYNC-MAP**, for **SYNC-MAP** we first prove that it is computationally intractable (*i.e.*, NP-hard) in terms of the number of nodes, by reducing it to the problem of the Exact Cover by 3-sets. The hardness is due to the fact that the cost structure of **SYNC-MAP** depends on the diameter of the resulting tree which is the ‘global’ information involving the entire topology. As a practical solution, we propose a polynomial-time greedy heuristic to recover a sub-optimal, but cost-efficient data graph.
- (c) Finally, for both **ASYNC-MAP** and **SYNC-MAP**, we quantify how the probability that the resulting (cost-efficient) data graph for a finite number of n samples differs from the ideal data graph decays as n increases, using the large deviation principle (LDP), as a form of $\exp(-n \cdot K)$. The error exponent K is characterized for each of **ASYNC-MAP** and **SYNC-MAP** by some topological information of physical/data graphs, cost structure for both inference mechanisms, and the degree of the trade-off. We validate our theoretical findings through simulations over a 20-node graph for a variety of scenarios and show their good match with the simulation results.

To validate our theoretical results, we perform numerical simulations a pair of physical and data graphs with 20 nodes, where we quantitatively analyze (i) how estimating a data graph considering communication cost affects the resulting estimation for various values of trade-off parameters between inference accuracy and cost, (ii) how the estimation error decays as the same size increases.

1.1 Related Work

A variety of applications which involve distributed in-network statistical inference tasks among spatially inter-connected agents or sensors have been widely studied in many online/offline systems. In sensor networks, where the knowledge of statistical dependencies among sensed data is given, the tasks of target tracking [20, 21, 22], detection [23], parameter estimation [24, 2] are the examples, see [4] for a survey. In social networks, where the underlying social phenomenon of interest such as voting models, rumor/opinion propagation [7] evolves over a given social interaction graph, the inference tasks of distributed consensus-based estimation [6], de-anonymization of community-structured social network [8] and distributed observability [5] are studied. Message-passing has manifested as an efficient procedure for inference over graphical models that provide the framework of succinct model of the statistical uncertainty of multi-agents. Examples include belief propagation (BP) [9], max-product [12, 10] and references therein. They are known to be exact and efficient when the underlying graphical model is a tree [9, 11]. Recent research progress has been made for scalable message-passing for general graphs, *e.g.*, junction tree [25] and graphs with loops [26].

In the area of structure learning, several algorithms have been proposed in the literatures to recover the statistical dependencies from a set of data samples [13, 14, 15, 16]. It is known that the exact structure learning for general graphical models is NP-hard. The research of structure learning for special graphical models includes: maximum likelihood estimation (MLE) [17, 16] for tree graphs, ℓ_1 regularized MLE for binary undirected graphs [13], convexified MLE for Gaussian graphical models, known as Lasso [14]. Theoretical guarantees for the learning accuracy have been established as the number of data samples, *e.g.*, on tree graph [27], on binary undirected graphs [13], on a class of Ising model [28], or on Bayesian network [29]. Our work differs from all of the above works in that we consider physical communication cost incurred by some target inference algorithms when learning the data dependency graph.

There exists an array of work that addresses the trade-off between inference quality and cost in running distributed in-network inference on the known data graph, which are summarized as two directions: (i) developing novel inference algorithms with less communication of messages or (ii) constructing a new graphical model upon which the existing distributed in-network inference algorithms are performed with less communication resources. In (i), the need of conserving resources requires to propose new message-passing schemes where the messages are compressed by allowing some approximation error in message values [21, 30, 26, 31], and/or some messages are censored (*i.e.*, not to be transmitted) [20]. In (ii), most of the related works focused on constructing a junction tree that minimizes the inference cost [3], building a data dependency structure upon which message-passing is run energy-efficiently, where the communications among all agents are assumed to be done in one-hop [1], or optimizing the data dependency structure formulated by a multi-objective problem of inference quality and energy, assuming that the exact statistical dependencies are given as a complete graph [32]. While the main interest of this area has been focused on characterizing the desirable dependency structure for given complete knowledge of accurate data dependencies, our work is motivated by the practical situation where one can just be

able to observe a finite number of data sample vectors of nodes, which do not provide such a complete knowledge. Therefore, our interest lies in *learning* the desirable data dependencies from a finite number of data samples.

2 Model and Preliminary

2.1 Model

Physical graph. We consider a (connected) physical network $G = (V, E_P)$ with a set of d nodes V and links E_P , where each node corresponds to an agent such as a sensor or an individual, and each link corresponds to a physical connectivity between two nodes. For example, in sensor networks, when nodes have wireless radios, then each link is established when two corresponding nodes over the link reach each other within each radio's communication range.

Data samples. Each node $i \in V$ generates a binary data, denoted by $x_i \in \mathcal{X} := \{0, 1\}^1$, where we denote by $\mathbf{x} = [x_i]_{i \in V}$ the data vector of all nodes, or simply a *sample*, e.g., target locations measured by all sensors. The underlying statistical uncertainty of samples can be represented by a joint distribution $P(\mathbf{x})$ of a random vector $X := [X_i]_{i \in V} \in \mathcal{X}^d$, called *data distribution*, where each random variable X_i is associated to each node $i \in V$. We often collect n multiple samples ($\mathbf{x}^{1:n} = \{\mathbf{x}^1, \mathbf{x}^2, \dots, \mathbf{x}^n\}$) in order to infer what happens in the network by understanding the inter-dependence of data generated by nodes. For instance, when sensors measure the target location, then we infer the underlying statistical correlation among sensors from the observed samples, to estimate the true target location.

Data graph via graphical model. The underlying statistical dependency is often understood by the framework of *graphical model*, which has been a popular tool for modeling uncertainty by a graph structure, where each node corresponds to a random variable and each edge captures the probabilistic interaction between nodes. In particular, we model the data distribution $P(\mathbf{x})$ as an undirected graph $T = (V, E_D)$, which we call *data graph*, which consists of the same set V of nodes as that in the physical graph and nodes' statistical dependencies captured by an edge structure E_D as: any two non-adjacent random variables are conditionally independent given all other variables, i.e., for any $(i, j) \notin E_D$,

$$P(x_i, x_j \mid x_{V \setminus \{i, j\}}) = P(x_i \mid x_{V \setminus \{i, j\}}) \cdot P(x_j \mid x_{V \setminus \{i, j\}}). \quad (1)$$

In this paper, we limit our focus on the tree-structured data graph (thus simply data tree), for which let \mathcal{T} and $\mathcal{P}(\mathcal{X}^d)$ be set of all spanning trees and set of all tree data distributions over V , respectively, i.e., we assume $T \in \mathcal{T}$ and $P \in \mathcal{P}(\mathcal{X}^d)$. Tree data graph is a class of graphical models that has received considerable attention in literatures [17, 19], since it possesses the following factorization property:

$$P(\mathbf{x}) = \prod_{i \in V} P_i(x_i) \prod_{(i, j) \in E_D} \frac{P_{i, j}(x_i, x_j)}{P_i(x_i) P_j(x_j)}, \quad (2)$$

¹We assume a binary data for simplicity, and our results are readily extended to any finite set \mathcal{X} .

where P_i and $P_{i,j}$ are the marginals on node $i \in V$ and edge $(i, j) \in E_D$, respectively. Tree-structured data graph is known to strike a good balance between the expressive power and the computational tractability. In particular, the distribution P in (2) is completely specified only by the set of edges E_D and their pairwise marginals. Thus, if P has the factorization property as in (2), in other words, if $P \in \mathcal{P}(\mathcal{X}^d)$, there exists a unique tree $T = T(P)$ corresponding to P . To abuse the notation, we henceforth denote by $T(P)$ the unique data tree of a tree distribution P . Figure 1 shows an example of the physical graph and two data graphs with 7 nodes.

2.2 Goal: Cost-efficient Learning of Data Graph

Learning data graph: What and why? To understand the underlying data dependency (2), it is enough to learn the structure of data graph E_D from the observed samples, which is known as the problem of *(data graph) structure learning*. Formally, when we are given a set of i.i.d. n samples $\mathbf{x}^{1:n}$ generated from an unknown (tree) data distribution $P \in \mathcal{P}(\mathcal{X}^d)$ on a data tree T , a *structure learning* algorithm is a (possibly randomized) map ϕ defined by:

$$\phi : (\mathcal{X}^d)^n \mapsto \mathcal{T}.$$

The quality of this algorithm $\hat{T} = \phi(\mathbf{x}^{1:n})$ is evaluated by how “close” \hat{T} is to the original data graph T .

Distributed inference on data graph. One of the practical goals of estimating the data tree given a set of data samples is to perform an inference task based on T . Thus, in many applications, primary interests are not focused on data itself but rather on how to exploit the data dependency for reliable decision making, such as target tracking, detection, estimation in sensor networks and/or social networks, which involves statistical inference about the networks described by a data graph. One example of inference tasks is the MAP (maximum a posteriori) based estimation. Distributed in-network inference has been widely studied with the help of various distributed algorithms on graphical models using *message-passing*. In particular, for a specific inference problem, a message between two nodes contains the information on influence that one node exerts on another, which is obtained based on the value contained in neighboring messages over an estimated data graph \hat{T} . One critical issue of message-passing based inference algorithm is that *messages are often passed along the multi-hop path on the physical graph G* , which incurs some amount of *communication cost*. Then, assuming that some inference algorithm would be run for the estimated data graph \hat{T} , such a data graph learning must have the trade-off between the accuracy of the learnt graph (*i.e.*, how close the learnt graph is to the original data graph) and the communication cost generated by performing the distributed inference.

Goal: Cost-efficient data graph learning. Given an observed samples $\mathbf{x}^{1:n}$ from the unknown data distribution P , our objective is to estimate a cost-efficient data tree, which captures the trade-off between (i) *inference accuracy* and (ii) *communication cost for inference*. For tree distributions, finding a distribution naturally gives rise to the corresponding data tree, as mentioned earlier. Thus, it is natural to find the tree distribution $\hat{Q}^*(n) = \hat{Q}^*(\mathbf{x}^{1:n}, G, \Pi, \gamma)$ that is the solution of the following optimization

problem: for a constant parameter $\gamma \geq 0$ and a fixed inference algorithm Π ,

$$\mathbf{CDG}(n) : \hat{Q}^*(n) = \arg \min_{Q \in \mathcal{P}(\mathcal{X}^d)} D(\hat{P}(\mathbf{x}^{1:n}) \parallel Q) + \gamma C(T(Q); G, \Pi), \quad (3)$$

where $\hat{P}(\mathbf{x}^{1:n}) := \frac{1}{n} \sum_{k=1}^n \mathbb{1}\{\mathbf{x}^k = \mathbf{x}\}$ is the empirical distribution of $\mathbf{x}^{1:n}$, $D(\cdot \parallel \cdot)$ is some distance metric between two distributions, and $C(T(Q); G, \Pi)$ is the communication cost paid by running an inference algorithm Π with respect to the data tree $T(Q)$ over the physical graph G . Recall that $T(Q)$ is the data tree for the tree distribution Q . The value of γ parameterizes how much we prioritize the communication cost compared to the inference accuracy $D(\hat{P}(\mathbf{x}^{1:n}) \parallel Q)$. Note that as $n \rightarrow \infty$, $\hat{P}(\mathbf{x}^{1:n})$ converges to the original data distribution P , which requires to solve $\mathbf{CDG}(\infty)$.

Then, this paper aims at answering the following two questions:

- (a) What are good data-tree learning algorithms that compute $T(\hat{Q}^*(n))$ by solving $\mathbf{CDG}(n)$? In Section 3, we consider the MAP estimator as an applied inference algorithm, and their two implementations having different cost functions, for which we propose two cost-efficient learning algorithms.
- (b) How fast does $\hat{Q}^*(n)$ converge to $\hat{Q}^*(\infty)$ as the number of samples n grows? We use the large deviation principle (LDP) to characterize the decaying rate of the probability that $T(\hat{Q}^*(n)) \neq T(\hat{Q}^*(\infty))$ for two different MAP implementations in Section 3.

In this paper, we use the popular KL divergence as a distance metric $D(\cdot \parallel \cdot)$ for inference accuracy, denoted by D_{KL} , where for two distributions P and Q , $D_{\text{KL}}(P \parallel Q) := \sum_{\mathbf{x} \in \mathcal{X}^d} P(\mathbf{x}) \log \frac{P(\mathbf{x})}{Q(\mathbf{x})}$. For notional simplicity, we simply denote by $Q^* := \hat{Q}^*(\infty)$ the solution of $\mathbf{CDG}(\infty)$ throughout this paper.

3 Cost-efficient Data Graph Learning Algorithms

In this paper, out of many possible inference tasks, we consider the maximum a posteriori (MAP) estimation, which is popularly applied in many applications such as data association for a multi-target tracking problem in sensor networks, community-structured social network de-anonymization problem in social networks [8].

3.1 Distributed MAP and Cost

Distributed MAP on tree-structured data graph. The MAP estimator of some tree distribution $Q \in \mathcal{P}(\mathcal{X}^d)$ on its associated data tree $T(Q) = (V, E_Q)$ is given by:

$$\mathbf{x}^{\text{MAP}} := \arg \max_{\mathbf{x} \in \mathcal{X}^d} \prod_{i \in V} \psi_i(x_i) \prod_{(i,j) \in E_Q} \psi_{i,j}(x_i, x_j), \quad (4)$$

where we use $\psi_i(x_i) = Q_i(x_i)$ and $\psi_{i,j}(x_i, x_j) = \frac{Q_{i,j}(x_i, x_j)}{Q_i(x_i)Q_j(x_j)}$ for simplicity. A standard message-passing algorithm for the distributed MAP is a max-product algorithm, which defines a message $m_{i \rightarrow j}^{(t)}(\cdot)$ from node i to j at t -th iteration with $(i, j) \in E_Q$.

Each node exchanges messages with their neighbors on the data tree $T(Q)$, and these messages are updated over time in an iterative fashion by the following rule: at t -th iteration,

$$m_{i \rightarrow j}^{(t+1)}(x_j) := \kappa \cdot \max_{x_i \in \mathcal{X}} \left[\psi_i(x_i) \psi_{i,j}(x_i, x_j) \prod_{k \in \mathcal{N}(i) \setminus \{j\}} m_{k \rightarrow i}^{(t)}(x_i) \right], \quad (5)$$

with the normalizing constant κ to make the sum of all message values be 1, and $\mathcal{N}(i)$ denotes the neighboring nodes of i .

Communication cost of distributed MAP. The communication cost of MAP is paid, depending on the actual protocol that specifies how to schedule message-passing procedures. Two natural message-passing protocols studied in literatures are: (a) asynchronous depth-first (unicast) update [33] and (b) synchronous (broadcast) parallel update [9]. Both protocols for a tree distribution Q with its data tree $T(Q)$ have been shown to be consistent in that the message update (5) converges to a unique fixed point $\{m_{i \rightarrow j}^*, m_{j \rightarrow i}^*\}_{(i,j) \in E_Q}$, which defines the exact MAP assignment in (4) as $x_i^{\text{MAP}} = \kappa \cdot \psi_i(x_i) \prod_{k \in \mathcal{N}(i)} m_{k \rightarrow i}^*(x_i)$ for each $i \in V$. We denote the cost of a single message-passing over an edge $e = (i, j)$, under a given physical graph G , as c_e or $c_{i,j}$. Recall that the message passing over $e = (i, j)$ may need to be done over a multi-hop path on the physical graph G . One simple example of $c_{i,j}$ is the shortest path distance from node i to j in G . Then, both protocols incur the communication cost as elaborated in what follows:

- (a) *Asynchronous*: In the *asynchronous* protocol (simply **ASYNC-MAP**), one node is arbitrarily picked as a root, and messages are passed from the leaves upwards to the root, then back downwards to the leaves. It involves a total $|E_Q|$ number of messages upon termination. Thus, the communication cost would be:

$$C(T(Q); G, \text{ASYNC-MAP}) = \sum_{(i,j) \in E_Q} 2c_{i,j}. \quad (6)$$

- (b) *Synchronous*: In the *synchronous* protocol (simply **SYNC-MAP**), at each iteration, every node sends messages to all of its neighbors. Then, since the diameter $\text{diam}(T(Q))^2$ is the minimum amount of time required for a message to pass between two most distant nodes in $T(Q)$, this protocol involves at most $\text{diam}(T(Q))$ iterations with total $2|E_Q| \cdot \text{diam}(T(Q))$ number of messages. Thus, we have the following cost:

$$C(T(Q); G, \text{SYNC-MAP}) = \sum_{(i,j) \in E_Q} 2c_{i,j} \cdot \text{diam}(T(Q)). \quad (7)$$

In the next subsection, we will use the above two cost functions for two different learning algorithms for **CDG(n)** in (3) to estimate two cost-efficient data trees.

²For a tree T with d nodes, $2 \leq \text{diam}(T) \leq d - 1$.

Algorithm 1: ASYNC-ALGO

Input: $\mathbf{x}^{1:n}$: a set of n samples, γ : the trade-off parameter, a physical graph $G = (V, E_P)$

Output: Estimated tree $T = (V, E)$.

S0. $E = \emptyset$ and for each possible edge $e \in V \times V$, we initialize its weight by:

$$w_e = I_e(\hat{P}) - 2\gamma \cdot c_e, \quad (9)$$

where $I_e(\mu)$ is the mutual information between two end-points of edge e with respect to a given joint distribution μ .

S1. Run a maximum weight spanning tree algorithm for H , and save its resulting spanning tree at $T = (V, E)$.

S2. Return T .

3.2 Algorithm for Asynchronous MAP

Using the cost function for the asynchronous MAP in (6), the original optimization problem **CDG**(n) is re-cast into:

$$\begin{aligned} \mathbf{CDG-A}(n) : \hat{Q}^*(n) = \\ \arg \min_{Q \in \mathcal{P}(\mathcal{X}^d)} D_{\text{KL}}(\hat{P}(\mathbf{x}^{1:n}) \parallel Q) + \gamma \sum_{e \in E_Q} 2c_e. \end{aligned} \quad (8)$$

We now describe **ASYNC-ALGO** that computes $\hat{Q}^*(n)$ in (8) and thus estimates the cost-efficient data tree $T(\hat{Q}^*(n))$ in Algorithm 1. As we see, the algorithm is remarkably simple. Using given n data samples, we construct a weighted complete graph, where the weight for each edge is assigned some combination of the mutual information of nodes i and j with respect to the empirical distribution \hat{P} obtained from the data samples and the per-message cost, as in (9). Then, we run an algorithm that computes the maximum weight spanning tree, *e.g.*, Prim's algorithm or Kruskal's algorithm, and the resulting spanning tree is the output of this algorithm.

Correctness of ASYNC-ALGO. We now present the correctness of the above algorithm in the sense that we can obtain the data tree corresponding to the optimal distribution formulated in (8), as explained in what follows: For some tree distribution Q (thus, satisfying the factorization property in (2)), we have:

$$\begin{aligned} D_{\text{KL}}(\hat{P} \parallel Q) &= -H(\hat{P}) - \sum_{\mathbf{x} \in \mathcal{X}^d} \hat{P}(\mathbf{x}) \log Q(\mathbf{x}) \\ &\geq -H(\hat{P}) + \sum_{i \in V} H(\hat{P}_i) - \sum_{(i,j) \in E_Q} I(\hat{P}_{i,j}), \end{aligned} \quad (10)$$

where $H(\cdot)$ is the entropy, and the inequality holds when the pairwise marginals over the edges of a fixed E_Q are set to that of \hat{P} , *i.e.*, $Q_{i,j}(x_i, x_j) = \hat{P}_{i,j}(x_i, x_j)$ for all

$(i, j) \in E_Q$. Since the entropy terms are constant w.r.t. Q , it is straightforward that the structure of the estimator $\hat{Q}^*(n)$ of **CDG-A**(n) in (8) is given by:

$$\hat{E}^*(n) := \arg \max_{E_Q: Q \in \mathcal{P}(\mathcal{X}^d)} \sum_{e \in E_Q} I_e(\hat{P}) - 2\gamma \cdot c_e, \quad (11)$$

$$\hat{Q}_{i,j}^*(n) = \hat{P}_{i,j}, \quad \forall (i, j) \in \hat{E}^*(n). \quad (12)$$

Then, it is easy to see that (11) requires us to find the maximum weight spanning tree using $I_e(\hat{P}) - 2\gamma \cdot c_e$ as the edge e 's weight, where the standard maximum weight spanning tree (MWST) computation algorithm runs in $O(d^2 \log d)$ time, where recall that $|V| = d$.

3.3 Algorithm for Synchronous MAP

Similarly to **ASYN-C-MAP**, using the cost in (7), the original optimization problem **CDG**(n) is re-cast into:

$$\begin{aligned} \mathbf{CDG-S}(n) : \hat{Q}^*(n) = \\ \min_{Q \in \mathcal{P}(\mathcal{X}^d)} D_{\text{KL}}(\hat{P}(\mathbf{x}^{1:n}) \parallel Q) + \gamma \cdot \text{diam}(T(Q)) \sum_{e \in E_Q} 2c_e. \end{aligned} \quad (13)$$

Following the similar arguments in Section 3.2, the structure of the above estimator of **CDG-S**(n) in (13) is given by

$$\hat{E}^*(n) := \arg \max_{E_Q: Q \in \mathcal{P}(\mathcal{X}^d)} \sum_{e \in E_Q} I_e(\hat{P}) - 2\gamma \text{diam}(T(Q)) \cdot c_e, \quad (14)$$

$$\hat{Q}_{i,j}^*(n) = \hat{P}_{i,j}, \quad \forall (i, j) \in \hat{E}^*(n). \quad (15)$$

We comment that this optimization is non-trivial in that the objective function contains the diameter of the tree, which can be computed only when the solution is fully characterized.

Hardness. The key difference in the cost function of **SYNC-MAP** from **ASYN-C-MAP** is simply the existence of $\text{diam}(T(Q))$. However, this simple difference completely changes the hardness of learning the optimal data tree in **SYNC-MAP**, as formally stated in the next Theorem.

Theorem 1 (Hardness of **CDG-S**(n)). *For any parameter $\gamma \geq 0$, obtaining the optimal distribution $\hat{Q}^*(n)$ in **CDG-S**(n) and thus its associated data tree $T(\hat{Q}^*(n))$ is NP-hard with respect to the number of nodes.*

Proof sketch. Due to space limitation, we present the full proof of Theorem 1 in Appendix A.1, and we only provide its sketch here. The key step in proof is to reduce the **CDG-S**(n) in (13) to the well-known NP-complete problem: *Exact Cover by 3-sets* problem, which we simply call **X3C**. In [34], the bounded diameter minimum weight spanning tree (BDMST) problem that finds the MWST with a diameter less than k of

$4 \leq k \leq |V| - 2$ for a fixed edge weights is shown to be an NP-hard problem, by reducing it to the **X3C** problem. The main technical challenge in **CDG-S**(n) lies in that the edge weights are *diameter-dependent*, via the form of $I_e(\hat{P}) - 2\gamma \cdot \text{diam}(T(Q)) \cdot c_e$ in (14), where the weights become smaller as the diameter $\text{diam}(T(Q))$ grows. Therefore, the optimal structure of $\hat{E}^*(n)$ in (14) would be attained at the tree with small diameter. If we consider a fixed diameter $\text{diam}(T(Q)) = k$ of $4 \leq k \leq |V| - 2$ so that the edge weights are set by constant values, then the problem becomes similar to the BDMST problem. To prove NP-hardness of our problem, we first construct a specific tree distribution $\bar{P}(\mathbf{x})$ and the cost functions $\{\bar{c}_{i,j}\}_{(i,j) \in V \times V}$, at which the optimal solution of **CDG-S**(n) should have a certain diameter, a diameter of 4 in our proof, then we show that **CDG-S**(n) for the weights of diameter 4 has the optimal solution with diameter 4 if and only if **X3C** problem has a solution. From understanding the reduction of BDMST problem, we construct $\bar{P}(\mathbf{x})$ and $\{\bar{c}_{i,j}\}_{(i,j) \in V \times V}$, under which (i) the tree with diameter less than 3 does not attain optimal solution due to its structural limitations (to force the small diameter), and (ii) the edge weights for the diameter larger than 5 become too small to achieve optimal solution of **CDG-S**(n). The remaining technique to verify the reduction of our problem to the **X3C** problem follows the arguments in [34]. Then, we are done with the reduction.

Greedy algorithm. Due to the above-mentioned hardness, we propose a greedy heuristic algorithm that outputs the tree structure denoted by $\hat{E}^S(n)$, called **SYNC-ALGO**(β), as we describe in Algorithm 2, where β is the algorithm parameter. The overall algorithm operates as follows:

- S0.** Initialize the weight of each possible edge with some initial value.
- S1.** Sequentially select the edge that has the maximum weight and add it to the temporary resulting tree.
- S2.** Update the weight of each edge whose one end-point is in the current resulting tree V_S and another end-point is not, and go to **S1** until we handle all nodes.

One of the central steps here is: first, we *dynamically* update the weight of the candidate edges (*i.e.*, the set E') that we will add and, second, which value is chosen as the weight is different from the “one-shot” weight assignment as done in **ASYN-ALGO**. To explain this intuition, we first note that from (14) it is easy to see that the degree of contribution in terms of weight by adding an edge $e \in E'$ to the existing resulting tree would be re-expressed as:

$$I_e(\hat{P}) - 2\gamma \text{diam}(T \cup \{e\}) \cdot c_e - K_e(T), \quad (20)$$

where $K_e(T)$ is defined in (18). Here, $K_e(T)$ corresponds to the change of the communication cost over the existing edges in T , under the grown tree $T \cup \{e\}$. For example, $K_e(T) = 0$ if the diameter of the grown tree does not change by adding the edge e , or $K_e(T) = \sum_{e' \in E_S} 2\gamma \cdot c_{e'}$, if the diameter of the grown tree increases by 1.

In dynamically assigning the weight of the candidate edges in E' , we do not use the value of (20). Instead, as seen in (17), (i) we use the expected diameter growth of the tree, denoted by $D(T)$ in (19), and (ii) we use a tunable parameter $\beta > 0$ to compensate for the impact of the change in communication cost over the existing edges $K_e(T)$ in (18). In more detail, we use $D(T)$ in (19), which captures the expected diameter growth

Algorithm 2: SYNC-ALGO(β)

Input: $x^{1:n}$: a set of n samples from P , γ : the trade-off parameter, a physical graph $G = (V, E_P)$, and a tunable parameter β .

Output: Estimated tree $T = (V_S, E_S)$.

S0. $V_S = \emptyset, E_S = \emptyset$, and for each possible edge $e \in V \times V$, we initialize its weight by:

$$w_e = I_e(\hat{P}) - 2\gamma \cdot c_e, \quad (16)$$

and initialize the edge set E' by the set of all possible edges.

repeat

S1. Select an edge $e = (u, v) \in E'$ with the maximum weight, and update $V_S \leftarrow V_S \cup \{u, v\}$ and $E_S \leftarrow E_S \cup \{e\}$.

S2. Update E' as the set of all edges $e = (i, j)$, such that $i \in V_S$ and $j \in V \setminus V_S$, and set the weight of each edge $e = (i, j) \in E'$ as:

$$w_e = I_e(\hat{P}) - 2\gamma \text{diam}(T \cup \{e\}) \cdot c_e - \beta \frac{d}{|E_S|} \cdot K_e(T) - 2\gamma \cdot D(T) \cdot c_e, \quad (17)$$

where

$$K_e(T) = \left(\text{diam}(T \cup \{e\}) - \text{diam}(T) \right) \cdot \sum_{e' \in E_S} 2\gamma \cdot c_{e'}, \quad (18)$$

and

$$D(T) = \sqrt{d} \cdot \left(1 - \frac{\sqrt{|E_S|}}{\sqrt{d}} \right). \quad (19)$$

until $V_S = V$;

Return $T = (V_S, E_S)$.

of the tree T via the term $\sqrt{d}(1 - \frac{\sqrt{|E_S|}}{\sqrt{d}})$, since the diameter of a uniformly random spanning tree is known to be of the order \sqrt{d} in [35]. We note that this term decreases to 0 as the tree becomes to a spanning tree from the term $1 - \frac{\sqrt{|E_S|}}{\sqrt{d}}$. Second, we consider the impact of old weights over the existing edges in T , captured by $K_e(T)$ in (20), by controlling a scale of $\beta \frac{d}{|E_S|}$.

To summarize, these two modified choices of the weight are for handling a probable sacrifice of the performance when using a vanilla greedy method as in (18), since the edge weight should be modified suitably for the changed diameter on the way of tree

construction. We expect that these two engineerings play an important role when the cost-efficient data graph is attained with a large diameter, where the edges chosen in the begging phase of the procedure (*i.e.*, with a small diameter value) could exert much impact of communication cost at the end of the procedure. Our greedy algorithm runs in $O(d^4)$ times.

4 Estimation Error for Increasing Sample Size

In this section, we provide the analysis of how the estimation error probability decays with the growing number of samples n , using the large deviation principle (LDP).

4.1 Estimation Error of ASYNC-ALGO

Clearly, when we use more and more data samples, $\hat{E}^*(n)$ approaches to $\hat{E}^*(\infty)$ that is the optimal edge structure solving $\mathbf{CDG-A}(\infty)$. We are interested in characterizing the following error probability of the event \mathcal{A}_n :

$$\mathbb{P}[\mathcal{A}_n(\mathbf{x}^{1:n}) := \{\hat{E}^*(n) \neq \hat{E}^*(\infty)\}]. \quad (21)$$

To characterize the probability in (21) that is one of the rare events, we use LDP that *rare events occurs in the most probable way*. To this end, we aim at studying the following rate function $K = K(\gamma)$:

$$K(\gamma) := \lim_{n \rightarrow \infty} -\frac{1}{n} \log \mathbb{P}(\mathcal{A}_n(\mathbf{x}^{1:n})), \quad (22)$$

whenever the limit exists.

We now consider a simple event, called *crossover event*, as defined in what follows: Recall that **ASYNC-ALGO** uses, for each edge e , the weight³ of $w_e(\hat{P}) = I_e(\hat{P}) - 2\gamma c_e$ based on the empirical distribution \hat{P} . Then, consider two edges e and e' such that the weight of e exceeds that of e' with respect to the *true* distribution P , *i.e.*, $w_e(P) > w_{e'}(P)$. We now define the crossover event for two edges e and e' as:

$$C_n(e, e') := \{w_e(\hat{P}) \leq w_{e'}(\hat{P})\}. \quad (23)$$

As the number of samples $n \rightarrow \infty$, the empirical distribution approaches to the true distribution, thus the probability of the crossover event decays to zero, whose decaying rate which we call *crossover rate* is defined as $J_{e,e'} := \lim_{n \rightarrow \infty} -\frac{1}{n} \log \mathbb{P}[C_n(e, e')]$. Using this definition of the crossover event, we present Theorem 2 that states the decaying rate of the estimation error probability as the number of data samples n grows.

Theorem 2 (Decaying rate of **ASYNC-ALGO**). *For any fixed parameter $\gamma \geq 0$,*

$$\lim_{n \rightarrow \infty} -\frac{1}{n} \log \mathbb{P}(\mathcal{A}_n(\mathbf{x}^{1:n})) = K(\gamma), \quad (24)$$

³We interchangeably use $w_e(\hat{P})$ to denote the assigned weight of an edge e in algorithms, with respect to the empirical distribution \hat{P} from the given samples.

where

$$K(\gamma) = \min_{e' \notin \hat{E}^*(\infty)} \min_{e \in \Psi(e'; \hat{E}^*(\infty))} J_{e,e'}, \quad (25)$$

where $\Psi(e' = (i, j); \hat{E}^*(\infty)) := \{v_1(= i), v_2, \dots, v_l(= j)\}$ is the unique path between nodes i and j , such that $(v_k, v_{k+1}) \in \hat{E}^*(\infty)$ for $1 \leq k \leq l-1$, and

$$J_{e,e'} = \begin{cases} \inf_{Q \in \mathcal{P}(\mathcal{X}^4)} \left\{ D_{KL}(Q \parallel P_{e,e'}) : w_e(Q) = w_{e'}(Q) \right\}, \\ \text{if } \{Q \in \mathcal{P}(\mathcal{X}^4) : w_e(Q) = w_{e'}(Q)\} \neq \emptyset, \\ \infty, \quad \text{otherwise.} \end{cases} \quad (26)$$

Moreover, we have the following (finite-sample) upper-bound on the error probability: for all $n = 1, 2, \dots$,

$$\mathbb{P}[\mathcal{A}_n(\mathbf{x}^{1:n})] \leq \frac{(d-1)^2(d-2)}{2} \binom{n-1+|\mathcal{X}|^4}{|\mathcal{X}|^4-1} \exp(-n \cdot K(\gamma)). \quad (27)$$

In Theorem 2, we observe that the decaying rate of error probability is specified by some topological information of physical/data graphs and the trade-off parameter γ . In particular, the crossover event and its rate $J_{e,e'}$ depend on how difficult it is to differentiate two edge weights under the true data distribution with a consideration of the trade-off parameter γ as well as per-message cost on edges. As interpreted from (26), when $w_e(P) = I_e(P) - 2\gamma c_e$ and $w_{e'}(P) = I_{e'}(P) - 2\gamma c_{e'}$ are close, the confusion between e and e' from samples frequently occurs, leading to high error probability, and we can show the existence of the infimum Q satisfying $w_e(Q) = w_{e'}(Q)$ as by slightly adjusting the true distribution P . Moreover, we remark that the decaying rate $J_{e,e'}$ (and thus $K(\gamma)$) is characterized by a trade-off parameter γ . The error rate becomes smaller (*i.e.*, higher error probability) when γ nearly meets the condition $w_e(P) = w_{e'}(P)$, and the weights becomes deterministic with respect to the samples as γ increases since the portion of the cost in weights grows, resulting to $J_{e,e'} = \infty$ in (26). These interpretations are well-matched to our numerical results in Section 5.

Proof sketch. The proof of Theorem 2 is presented in Appendix A.2, and we describe the proof sketch for readers' convenience. Our proof largely follows that of the related work in [27] that analyzes an error exponent of a standard tree structure learning (*i.e.*, known as Chow-Liu algorithm [17]), whose goal is to solely estimate the true data distribution with no consideration of communication cost. Simply, the proof idea follows LDP in the following way. The error event $\mathcal{A}_n(\mathbf{x}^{1:n})$ is expressed as a union of small events that **ASYNC-ALGO** estimates only one wrong edge (see the definition of the crossover event in (23)), two wrong edges, and three, etc. Following LDP, the decaying rate of the error probability equals to the decaying rate of the most probable crossover event, which corresponds to the case of only one wrong edge. In more detail, two minimums in (25) specify the most-probably error, whose edge set differs from the optimal data tree structure $\hat{E}^*(\infty)$ exactly in one edge, *i.e.*, $\hat{E}^*(\infty) \setminus \{e\} \cup \{e'\}$, where it contains the non-neighbor node pair e' (as selected in the first minimization) instead of

the most probable replacement edge e in the unique path along $\hat{E}^*(\infty)$ (as in the second minimization). To obtain the minimum crossover rate $J_{e,e'}$, we apply the Sanov's theorem [36], which provides an expression of the probabilistic relationship between \hat{P} and P via their KL divergence. Finally, in addition to the asymptotic decaying rate of the estimation error probability, we also establish its upper bound of the error probability in terms of the number n of data samples, where the first term $(d-1)^2(d-2)/2$ of the bound in (27) implies the number of possible crossover events, and the second term $\binom{n-1+|\mathcal{X}|^4}{|\mathcal{X}|^4-1}$ represents the number of possible empirical distributions $\hat{P}_{e,e'}$.

4.2 Estimation Error of SYNC-ALGO

We conduct a similar analysis here for **SYNC-ALGO** to what we did for **ASYN-ALGO**, which has more complicated issues for the following reasons: We first denote by $w_e(\hat{P}, T)$ in (17) the assigned weight for edge e to stress its dependence on the corresponding resulting tree structure T and its associated empirical distribution \hat{P} . Then, we need to investigate the most probable pattern in the rare event through a certain tree T at some iteration. Simply, the crossover event for two edges e and e' occurs if the order of edge weights from the given finite number of samples becomes reversed to the order of weights from the true data distribution. Among all possible crossover events, we are interested in the crossover event under every tree structure that is obtained on the way of constructing the ideal data structure, denoted by $\hat{E}^S(\infty)$. Let e_{true}^t and T_{true}^t be the selected edge and constructed tree at t -th iteration obtained by running **SYNC-ALGO** w.r.t. the true data distribution P , which would finally find $\hat{E}^S(\infty)$. Then, it is obvious that e_{true}^t has the unique highest edge weight for P , and the crossover event of our interest is defined as:

$$C_n(e_{\text{true}}^t, e'; T_{\text{true}}^t) := \left\{ w_{e_{\text{true}}^t}(\hat{P}; T_{\text{true}}^t) \leq w_{e'}(\hat{P}; T_{\text{true}}^t) \right\}. \quad (28)$$

We now state Theorem 3 that establishes the decaying rate of the estimation error probability as the number of data samples grows.

Theorem 3 (Decaying rate of **SYNC-ALGO**). *For any fixed parameter $\gamma \geq 0$,*

$$\lim_{n \rightarrow \infty} -\frac{1}{n} \log \mathbb{P}(\mathcal{A}_n(\mathbf{x}^{1:n})) \geq K(\gamma), \quad (29)$$

where

$$K(\gamma) := \min_{t \in \{1, \dots, |V|-1\}} \min_{e' \notin T_{\text{true}}^{t+1}} J_{e_{\text{true}}^t, e'}(T_{\text{true}}^t), \quad (30)$$

where e_{true}^t and T_{true}^t are the selected edge and constructed tree at t -th iteration by running **SYNC-ALGO** w.r.t. the true data distribution P , i.e., $w_{e_{\text{true}}^t}(P)$ has the maximum edge weight under the tree T_{true}^t , and it is given by: under some tree T , for any e, e' ,

$$J_{e,e'}(T) = \begin{cases} \inf_{Q \in \mathcal{P}(\mathcal{X}^4)} \left\{ D_{KL}(Q \parallel P_{e,e'}) : w_e(Q) = w_{e'}(Q) \right\}, \\ \quad \text{if } \{Q \in \mathcal{P}(\mathcal{X}^4) : w_e(Q) = w_{e'}(Q)\} \neq \emptyset, \\ \infty, \quad \text{otherwise.} \end{cases} \quad (31)$$

Moreover, we have the following (finite-sample) upper-bound on the error probability: for all $n = 1, 2, \dots$,

$$\mathbb{P}[\mathcal{A}_n(\mathbf{x}^{1:n})] \leq \frac{(d-1)d(d+1)}{6} \binom{n-1+|\mathcal{X}|^4}{|\mathcal{X}|^4-1} \exp(-n \cdot K(\gamma)). \quad (32)$$

In Theorem 3, as seen in (29), the error rate function $K(\gamma)$ in (30) indeed provides a lower-bound of the actual decaying rate of the error event $\mathcal{A}_n(\mathbf{x}^{1:n})$, since the crossover event $C_n(e_{\text{true}}^t, e'; T_{\text{true}}^t)$ which estimates an edge $e' \notin T_{\text{true}}^{t+1}$ rather than e_{true}^t at any t -th iteration does not guarantee that e' is a wrong edge. Intuitively, the edge weights of **SYNC-ALGO** dynamically change according to a diameter of T_{true}^t as iteration t proceeds, which makes the characterization of the exact error rate of **SYNC-ALGO** be non-trivial.

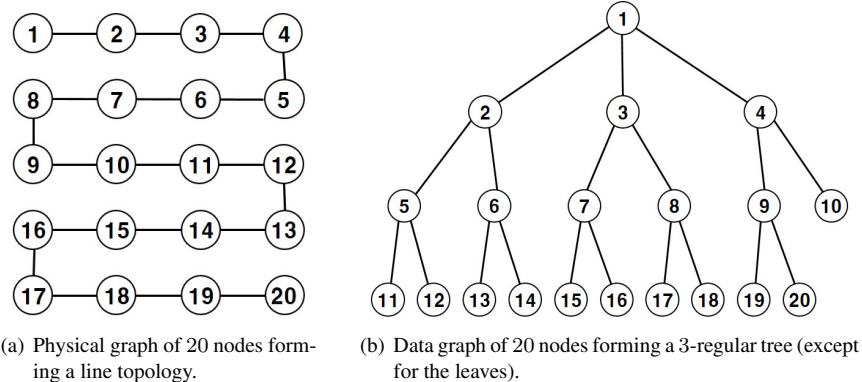
Proof sketch. Due to space limitation, we present the complete proof in Appendix A.3, and we provide a brief proof sketch. The basic idea is similar to the proof of Theorem 2. As mentioned there, the crossover event $C_n(e_{\text{true}}^t, e'; T_{\text{true}}^t)$ is not a subset of the error event $\mathcal{A}_n(\mathbf{x}^{1:n})$, and as a result, we provide a lower-bound of the decaying error rate in the proof, as established by two minimizations in (31). In particular, the first minimization is taken over all iterations ($1 \leq t \leq |V| - 1$) so that it selects the iteration where the error occurs in the most probable way, and the second minimization specifies the non-neighbor node pair e' , which can be estimated instead of e_{true}^t , having the minimum $J_{e_{\text{true}}^t, e'}(T_{\text{true}}^t)$. In other words, the most probable pattern in the error event of **SYNC-ALGO** is to estimate $T_{\text{true}}^t \setminus \{e_{\text{true}}^t\} \cup \{e'\}$ attained in two minimizations in (30). For the crossover rate $J_{e_{\text{true}}^t, e'}(T_{\text{true}}^t)$ in (31), when two edges e_{true}^t and e' can be clearly differentiated via their edge weights, since the difference of the cost between two edges dominantly determines the order of the edge weights, *i.e.*, the condition in (31) does not hold, the crossover event does not happen, *i.e.*, $J_{e_{\text{true}}^t, e'}(T_{\text{true}}^t) = \infty$. This mostly corresponds to the situation of a large value of the trade-off parameter γ , where the communication cost plays an important role of the error event, which do not depend on the number of samples n . Otherwise, the crossover rate is attained in a similar way to (26). Finally, we establish the upper bound of the error probability in terms of the sample size n , where the first term $(d-1)d(d+1)/6$ of the bound in (32) corresponds to the number of possible crossover events throughout the entire iterations, and the second term implies the number of possible empirical distributions $\hat{P}_{e_{\text{true}}^t, e'}$.

5 Numerical Results

In this section, we provide a set of numerical experiments to validate our analytical results of **ASYNC-ALGO** and **SYNC-ALGO** under various numbers of data samples, communication costs, and trade-off parameters.

5.1 Setup

Physical graph. We use a physical network $G = (V, E_P)$ consisting of 20 nodes forming a line topology, where node i can directly communicate only with nodes $i - 1$ and



$i+1$, see Figure 2(a). We assign some constant cost of single message-passing for each edge $e = (i, i+1)$: $c_{i,i+1} = \kappa \times 1.1^i$, except for $c_{1,2} = 4\kappa, c_{3,4} = 2\kappa, c_{6,7} = 0.1\kappa$, where we appropriately choose κ to adjust the scale of total communication cost of two learning algorithms in the same range, for clear comparison with the same values of γ . In the message-passing between non-neighboring (w.r.t. the physical graph) node pairs (i, j) , we simply assume that it expends the sum of the costs when it is passed along the unique shortest multi-hop path $\Psi((i, j); G)$ on G , i.e., $c_{i,j} = \sum_{e' \in \Psi((i,j); G)} c_{e'}$. For example, $c_{1,4} = c_{1,2} + c_{2,3} + c_{3,4}$. We use this line topology for an exemplar physical graph to clearly observe the difference between **ASync-ALGO** and **Sync-ALGO**, where it leads to a significantly huge amount of communication cost for **Sync-MAP**, due to large diameter value $\text{diam}(G) = 19$.

Data graph. As an underlying statistical dependencies among 20 nodes in the data graph, we consider a 3-regular tree $T = (V, E_D)$, except for boundary nodes, where the node 1 is a root node and every node has a degree of 3 or less, as depicted in Figure 2(b). Each random variable X_i associated to a node i is set to follow a Bernoulli distribution. For a root node 1, it has $P(X_1 = 0) = 0.7$ and $P(X_1 = 1) = 0.3$, and for other neighboring node pairs i and j , we set the conditional distribution between X_i and X_j by

$$P(X_i = 0|X_j = 0) = 0.7, \quad \text{and} \quad P(X_i = 0|X_j = 1) = 0.3 \quad (33)$$

whenever $i < j$. With this setting of per-node distribution, it turns out that neighboring node pairs have high correlations, and thus have distinct values of the mutual information.

Under this choice of physical and data graphs, we obtain numerical examples to show the performance of **ASync-ALGO** and **Sync-ALGO** for various values of trade-off parameter γ , ranging from 0 to 4, and a fixed $\beta = 1$ in our results. For a fixed $n \in \mathbb{N}$, we first generate n i.i.d. samples $\mathbf{x}^{1:n}$ from $P(\mathbf{x})$ in (33). Then, we compute the empirical distribution $\hat{P}(\mathbf{x}^{1:n})$ and the empirical mutual information of all possible node pairs $\{I_e(\hat{P})\}_{e \in V \times V}$. Then, we learn the cost-efficient data tree

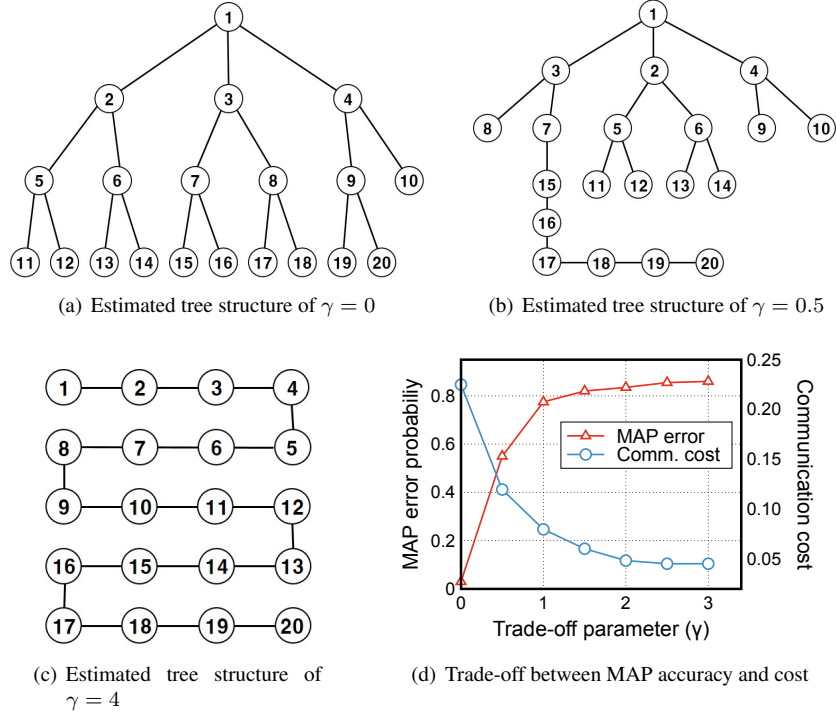


Figure 3: An instance of estimated tree structure by **ASync-ALGO** with distinct trade-off parameter $\gamma = 0, 0.5, 4$, and the trade-off between MAP accuracy and communication cost.

by running **ASync-ALGO** or **Sync-ALGO**, and estimate how well the proposed algorithms recover the ideal data graph by investigating the estimation error probability as n grows.

5.2 Results

(i) *Estimated trees with varying γ .* Figures 3 and 4 show that the estimated data trees by **ASync-ALGO** and **Sync-ALGO** for various γ . We recall that the value of γ parameterizes the amount of priority for communication cost compared to the inference quality, see (3), where smaller γ leads to higher priority to the inference quality. In both algorithms, we observe that they with $\gamma = 0$ estimate the exact data graph in Figure 2(b), since the goal is to achieve the highest inference accuracy. However, as γ grows, each of two algorithms estimates a different structure for data tree, since **ASync-MAP** and **Sync-MAP** have different forms of communication costs. In particular, in **ASync-ALGO**, as γ grows, we observe that the algorithm produces the estimated data tree with more resemblance to the physical graph, and finally it estimates the data tree that is the same as the physical graph with $\gamma = 4$, see Figures 3(b) and 3(c).

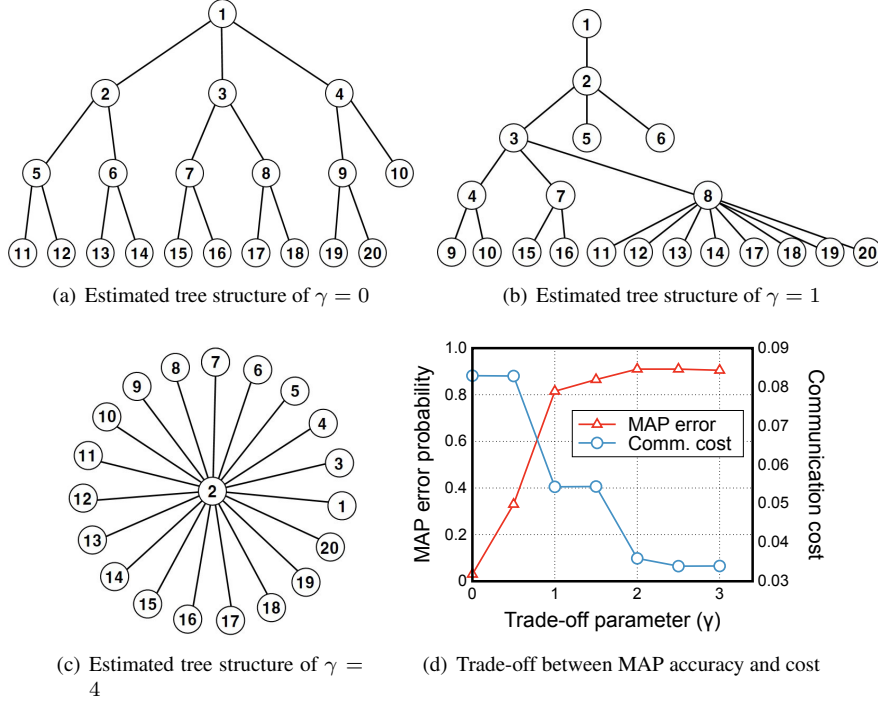


Figure 4: An instance of estimated tree structure by **SYNC-ALGO** with distinct trade-off parameter $\gamma = 0, 1, 4$, and the trade-off between MAP accuracy and communication cost.

We note that for a large value of γ , the goal of **ASYNC-ALGO** is to find a MWST of minimum total cost, which accords with the physical graph of line-topology. However, the communication cost of **SYNC-ALGO** increases in proportion to the *diameter* of the estimated tree, thus it estimates a tree that is of a *star-like* topology, *i.e.*, a tree with a small diameter as seen in Figures 4(b) and 4(c), to significantly reduce the cost, as γ grows.

(ii) **Quantifying trade-off between inference accuracy and cost.** We now quantify how the trade-off between inference accuracy of the MAP estimator in (4) behaves and the total communication cost is captured for different values of γ . To support the trade-off parameterized by γ in the optimization problem in (3), we vary γ from 0 to 4 and plot the accuracy of MAP estimator and the total cost on the learnt data dependency graph as the red and blue lines, respectively, in Figures 3(d) and 4(d). In particular, we run the **ASYNC-ALGO** and **SYNC-ALGO** with $n = 200$ samples, respectively, and run the max-product algorithm on the learnt data tree to obtain the MAP estimator. We repeatedly run for 200 times, and measure the error probability that the MAP estimator on the learnt data tree differs from the MAP estimator on the true data graph, as a metric of inference accuracy. The average (over the 200 results) of the communication

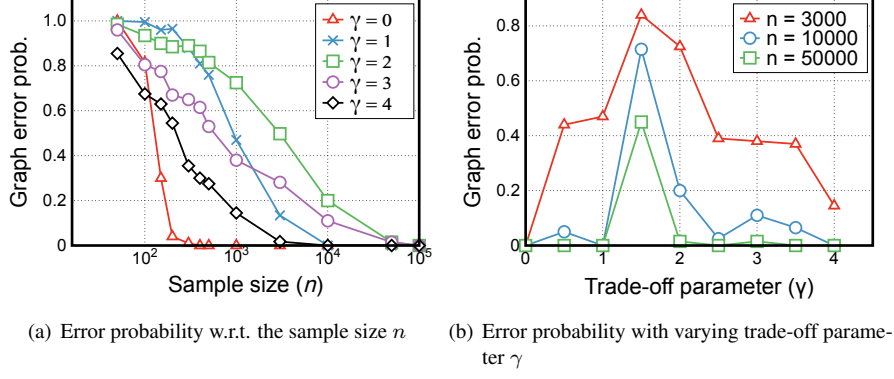


Figure 5: Error probability of **ASYNC-ALGO**.

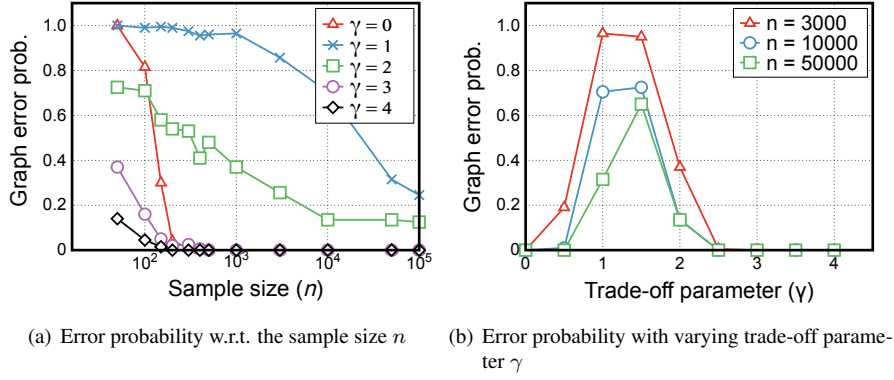


Figure 6: Error probability of **SYNC-ALGO**.

cost on the learnt data tree is measured by the form of (6) and (7) for each algorithm. In Figure 4(d), we observe that the MAP estimation error and cost with $\gamma = 0.5$ is 0.33 and 0.083, respectively, while those with $\gamma = 2.5$ is 0.91 and 0.034, respectively. The impact of γ on the trade-off for two algorithms seems similar, as seen in Figures 3(d) and 4(d).

(iii) Impact of data sample size on graph estimation accuracy. Finally, we demonstrate the theoretical findings in Theorems 2 and 3 on the decaying rate of the error probability w.r.t. the number of samples n for various values of γ . In both **ASYNC-ALGO** and **SYNC-ALGO**, for a fixed γ , we run both algorithms for 200 times each, and measure their error probabilities. In Figures 5(a) and 6(a), we observe that the error probability $\mathbb{P}(\mathcal{A}_n)$ for every γ decays exponentially as the sample size n increases, as established in (27) and (32). It is interesting to see that a different choice of γ leads to a different decaying rate, which can be understood by our analytical findings of the

crossover rate in (26) and (31), simply given by:

$$J_{e,e'}(T) = \inf_{Q \in \mathcal{P}(\mathcal{X}^4)} \left\{ D_{\text{KL}}(Q \parallel P_{e,e'}) : w_e(Q) = w_{e'}(Q) \right\},$$

where the edge weights for **ASync-ALGO** and **Sync-ALGO** are assigned in different forms, yet depending on the value of γ , as seen in (9) and (17). Some choice of γ makes a difference of the corresponding edge weights highly small, so that it becomes easier to estimate wrong edges with an insufficient number of samples. In our simulation, **ASync-ALGO** with $\gamma = 2$ shows higher error probability of 0.2 with $n = 10^4$ samples, while that with $\gamma = 0$ achieves almost 0 error probability with less than 3000 samples, see Figure 5(a). This impact of γ on the error probability is presented in Figures 5(b) and 6(b) for both algorithms, where for large γ , we observe the error probability decays at a higher rate in general, since the priority to the inference accuracy is insignificant, leading to less chance of experiencing the crossover event.

6 Conclusion

In many multi-agent networked systems, a variety of applications involve distributed in-network statistical inference tasks, such as MAP (maximum a posteriori), exploiting a given knowledge of statistical dependencies among agents. When agents are spatially-separated, running an inference algorithm leads to a non-negligible amount of communication cost due to inevitable message-passing, coming from the difference between data dependency and physical connectivity. In this paper, we consider a structure learning problem which recovers the statistical dependency from a set of data samples, which also considers the communication cost incurred by the applied distributed inference algorithms to the learnt data graph. To this end, we first formulate an optimization problem formalizing the trade-off between inference accuracy and cost, whose solution chooses a tunable point in-between them. As an inference task, we studied the distributed MAP and their two implementations **ASync-MAP** and **Sync-MAP** that have different cost generation structures. In **ASync-MAP**, we developed a polynomial time, optimal algorithm, inspired by the problem of finding a maximum weight spanning tree, while we proved that the optimal learning in **Sync-MAP** is NP-hard, thus proposed a greedy heuristic. For both algorithms, we then established how the error probability that the learnt data graph differs from the ideal one decays as the number of samples grows, using the large deviation principle.

References

- [1] Wei Zhao and Yao Liang. Energy-efficient and robust in-network inference in wireless sensor networks. *IEEE transactions on cybernetics*, 45(10):2105–2118, 2015.
- [2] Jeremy Schiff, Dominic Antonelli, Alexandros G Dimakis, David Chu, and Martin J Wainwright. Robust message-passing for statistical inference in sensor networks. In *International Symposium on Information Processing in Sensor Networks*, pages 109–118. IEEE, 2007.

- [3] Mark Paskin, Carlos Guestrin, and Jim McFadden. A robust architecture for distributed inference in sensor networks. In *International symposium on Information processing in sensor networks*, page 8. IEEE Press, 2005.
- [4] Venugopal V Veeravalli and Pramod K Varshney. Distributed inference in wireless sensor networks. *Philosophical Transactions of the Royal Society A*, 34(3):100–117, 2012.
- [5] Mohammadreza Doostmohammadian and Usman A Khan. Graph-theoretic distributed inference in social networks. *IEEE Journal of Selected Topics in Signal Processing*, 8(4):613–623, 2014.
- [6] Usman A Khan and Jose MF Moura. Distributing the kalman filter for large-scale systems. *IEEE transactions on signal processing*, 56(10):4919–4935, 2008.
- [7] Daron Acemoglu and Asuman Ozdaglar. Opinion dynamics and learning social networks. *Dynamic Games and Applications*, 1(1):3–49, 2011.
- [8] Xinze Fu, Zhongzhao Hu, Zhiying Xu, Luoyi Fu, and Xinbing Wang. De-anonymization of social networks with communities: When quantifications meet algorithms. *arxiv preprint arXiv:1703.09028*, 2017.
- [9] Judea Pearl. *Probabilistic reasoning in intelligent systems: networks of plausible inference*. Morgan Kaufmann, 2014.
- [10] Amir Globerson and Tommi S Jaakkola. Fixing max-product: Convergent message passing algorithms for map lp-relaxations. In *Advances in neural information processing systems*, pages 553–560, 2008.
- [11] Martin J Wainwright, Tommi S Jaakkola, and Alan S Willsky. Map estimation via greement on trees: message-passing and linear programming. *IEEE transactions on information theory*, 51(11):3697–3717, 2005.
- [12] Yair Weiss and William T Freeman. On the optimality of solutions of the max-product belief-propagation algorithm in arbitrary graphs. *IEEE transactions on information theory*, 47(2):736–744, 2001.
- [13] Pradeep Ravikumar, Martin J Wainwright, and John D Lafferty. High-dimensional ising model selection using 1-regularized logistic regression. *The Annals of Statistics*, 38(3):1287–1319, 2010.
- [14] Jerome Friedman, Trevor Hastie, and Robert Tibshirani. Sparse inverse covariance estimation with the graphical lasso. *Biostatistics*, 9(3):432–441, 2008.
- [15] Pieter Abbeel, Daphne Koller, and Andrew Y Ng. Learning factor graphs in polynomial time and sample complexity. *Journal of Machine Learning Research*, 7(Aug):1743–1788, 2006.
- [16] Marina Meila and Michael I Jordan. Learning with mixtures of trees. *Journal of Machine Learning Research*, 1(Oct):1–48, 2000.
- [17] C Chow and C Liu. Approximating discrete probability distributions with dependence trees. *IEEE transactions on Information Theory*, 14(3):462–467, 1968.
- [18] Sanjoy Dasgupta. Learning polytrees. In *Conference on Uncertainty in artificial intelligence*, pages 134–141. Morgan Kaufmann Publishers Inc., 1999.
- [19] Anima Anandkumar, Furong Huang, Daniel J Hsu, and Sham M Kakade. Learning mixtures of tree graphical models. In *Advances in Neural Information Processing Systems*, pages 1052–1060, 2012.
- [20] Lei Chen, Mujdat Cetin, and Alan S Willsky. Distributed data association for multi-target tracking in sensor networks. 2005.

- [21] Cetin Muijdat, Lei Chen, John W Fisher, Alexander T Ihler, Randolph L Moses, Martin J Wainwright, and Alan S Willsky. Distributed fusion in sensor networks. *IEEE Signal Processing Magazine*, 23(4):42–55, 2006.
- [22] Jianru Xue, Nanning Zheng, Jason Geng, and Xiaopin Zhong. Tracking multiple visual targets via particle-based belief propagation. *IEEE transactions on systems, man, and cybernetics, Part B (Cybernetics)*, 38(1):196–209, 2008.
- [23] Jean-Francois Chamberland and Venugopal V Veeravalli. Wireless sensors in distributed detection applications. *IEEE signal processing magazine*, 24(3):16–25, 2007.
- [24] Alexander T Ihler, John W Fisher, Randolph L Moses, and Alan S Willsky. Nonparametric belief propagation for self-localization of sensor networks. *IEEE Journal on Selected Areas in Communications*, 23(4):809–819, 2005.
- [25] Martin J Wainwright, Tommi S Jaakkola, and Alan S Willsky. Tree-based reparameterization framework for analysis of sum-product and related algorithms. *IEEE transactions on information theory*, 49(5):1120–1146, 2003.
- [26] Alexander T Ihler, W Fisher John III, and Alan S Willsky. Loopy belief propagation: Convergence and effects of message errors. *Journal of Machine Learning Research*, 6(May):905–936, 2005.
- [27] Vincent YF Tan, Animashree Anandkumar, Lang Tong, and Alan S Willsky. A large-deviation analysis of the maximum-likelihood learning of markov tree structures. *IEEE transactions on Information Theory*, 57(3):1714–1735, 2011.
- [28] Guy Bresler. Efficiently learning ising models on arbitrary graphs. In *Annual ACM on Symposium on Theory of Computing*, pages 771–782. ACM, 2015.
- [29] Or Zuk, Shiri Margel, and Eytan Domany. On the number of samples needed to learn the correct structure of a bayesian network. *arxiv preprint arXiv:1206.6862*, 2012.
- [30] O Patrick Kreidl and Alan S Willsky. Inference with minimal communication: A decision-theoretic variational approach. In *Advances in neural information processing systems*, pages 675–682, 2006.
- [31] Justin Dauwels. On variational message passing on factor graphs. In *IEEE International Symposium on Information Theory*, pages 2546–2550. IEEE, 2007.
- [32] Chongyu Zhou, Chen-Khong Tham, and Mehul Montani. Optimizing graphical model structure for distributed inference in wireless sensor networks. In *IEEE International Conference on Sensing, Communication, and Networking (SECON)*, pages 1–9. IEEE, 2016.
- [33] Gal Elidan, Ian McGraw, and Daphne Koller. Residual belief propagation: Informed scheduling for asynchronous message passing. *arxiv preprint arXiv:1206.6837*, 2012.
- [34] Michael R Garey and David S Johnson. *Computers and intractability*, volume 29. Springer-Verlag, Berlin, 2002.
- [35] A Rényi and G Szekeres. On the hieght of trees. *Journal of Autralian Mathematicl Society*, 7(4):497–507, 1967.
- [36] James A Bucklew. *Large deviation techniques in decision, simulation, and estimation*. Wiley New York, 1990.
- [37] Amir Dembo and Ofer Zeitouni. *Large deviations techniques and applications, volume 38 of Stochastic Modelling and Applied Probability*. Springer-Verlag, Berlin, 2010.

A Appendix

A.1 Proof of Theorem 1

To prove the NP-hardness of the problem **SYNC**(\mathbf{n}) in (13), we need some assumptions. Per-message communication cost satisfies following: (a) for all i, j , we have $c_{i,j} > 0$ and (b) for all distinct i, j, k , we have $c_{i,j} + c_{j,k} \geq c_{i,k}$. We assume that mutual information and communication cost are defined on the complete graph $\mathcal{G} = (\mathcal{V}, \mathcal{E})$. As we expressed in (??), for given $\mathbf{x}^{1:n}$, the objective function of a tree $T_Q \in \mathcal{T}$ for a fixed $\gamma \in \mathbb{R}_{\geq 0}$ is

$$\mathcal{O}^\gamma(T_Q, \hat{P}(\mathbf{x}^{1:n})) = \sum_{e \in \mathcal{E}_Q} I(\hat{P}_e) - 2\gamma D_{T_Q} \cdot c_e.$$

For convenience, we denote by $c_e^\gamma = 2\gamma c_e$ in the remaining of the paper. Then, the problem **SYNC**(\mathbf{n}) is equivalent to find a tree $T^\gamma(\mathbf{x}^{1:n}) = \arg \max_{T_Q \in \mathcal{T}} \mathcal{O}^\gamma(T_Q)$.

Proof. We reduce the problem **SYNC**(\mathbf{n}) in (13) to the known NP-complete problem *Exact Cover by 3-sets*, simply called **X3C** problem. We first describe what the **X3C** problem is.

Exact Cover by 3-sets (X3C). Given a set $S = \{1, 2, \dots, 3s\}$ of nodes and a set $F = \{f_1, f_2, \dots, f_q\}$ of 3-element subsets of S , **X3C** problem is the *decision problem* which determines that whether there exists $F' \subset F$ such that (i) the union of the elements of F' is S and (ii) the intersection of any two elements of F' is an empty set. It is known to be NP-complete.

To prove the NP-hardness of **SYNC**(\mathbf{n}) in (13), we build a specific (tree) data distribution $\bar{P}(x)$ with $T_{\bar{P}} = (\mathcal{V}, \mathcal{E}_{\bar{P}})$ for the $d = 3s + q + 3$ node variables in \mathcal{V} and a specific cost functions $\bar{c}^\gamma := \{\bar{c}_{i,j}^\gamma\}_{(i,j) \in \mathcal{V} \times \mathcal{V}}$, so that the corresponding optimization problem can be converted to the **X3C** problem. We prove that under such a specific situation, the diameter of the optimal tree in (??) should be 4 and we can solve the **X3C** problem if and only if we have optimal tree solution.

Construction of the joint distribution $\bar{P}(\mathbf{x})$. There are $3s + q + 3$ node variables in \mathcal{V} , where $X = \{X_1, \dots, X_{3s}\}$ denote the element nodes and $Y = \{Y_1, \dots, Y_q\}$ denote the subset nodes. The remaining three nodes are denoted by Z_0, Z_1 and Z_2 , i.e., $\mathcal{V} = X \cup Y \cup \{Z_0, Z_1, Z_2\}$. First, we construct a tree $T_{\bar{P}}$ (whose distribution would be defined below), where the node variable Z_0 is a root node and the subset nodes Y_1, \dots, Y_q are connected to Z_0 . Each subset node of Y is connected to the element nodes of X up to 3 nodes, and the element nodes are leaf nodes in the tree. Finally, Z_1 is connected to Z_0 and Z_2 and Z_2 has a single connection to Z_1 . It is obvious that $T_{\bar{P}}$ is a spanning tree with set of nodes \mathcal{V} , and there exist four kinds of edges in $\mathcal{E}_{\bar{P}}$: (i) (X_i, Y_j) for some $X_i \in X$ and $Y_j \in Y$, (ii) (Y_j, Z_0) for all $Y_j \in Y$, (iii) (Z_0, Z_1) and (iv) (Z_1, Z_2) , and finally its diameter is 4, i.e., $D_{T_{\bar{P}}} = 4$.

We now construct the tree distribution $\bar{P}(x)$ of the tree $T_{\bar{P}}$ as follows. For all node variables $v \in \mathcal{V}$, we set the marginal distribution as Bernoulli distribution with probability $\frac{1}{2}$. For marginal distribution of the edges, we set as follows: for (X_i, Y_j)

and $(Y_j, Z_0) \in \mathcal{E}_{\bar{P}}$,

$$\begin{aligned}\bar{P}(X_i = 0, Y_j = 0) &= \bar{P}(X_i = 1, Y_j = 1) = \frac{1}{4} + \frac{1}{2}\delta_d, \\ \bar{P}(X_i = 0, Y_j = 1) &= \bar{P}(X_i = 1, Y_j = 0) = \frac{1}{4} - \frac{1}{2}\delta_d, \\ \bar{P}(Y_j = 0, Z_0 = 0) &= \bar{P}(Y_j = 1, Z_0 = 1) = \frac{1}{4} + \frac{1}{2}\delta_d, \\ \bar{P}(Y_j = 0, Z_0 = 1) &= \bar{P}(Y_j = 1, Z_0 = 0) = \frac{1}{4} - \frac{1}{2}\delta_d,\end{aligned}\tag{34}$$

where δ_d is a positive constant determined by the number of nodes d . For remaining edges (Z_0, Z_1) and (Z_1, Z_2) , we set

$$\begin{aligned}\bar{P}(Z_0 = 0, Z_1 = 0) &= \bar{P}(Z_0 = 1, Z_1 = 1) = \frac{9}{10}, \\ \bar{P}(Z_0 = 0, Z_1 = 1) &= \bar{P}(Z_0 = 1, Z_1 = 0) = \frac{1}{10}, \\ \bar{P}(Z_1 = 0, Z_2 = 0) &= \bar{P}(Z_1 = 1, Z_2 = 1) = \frac{9}{10}, \\ \bar{P}(Z_1 = 0, Z_2 = 1) &= \bar{P}(Z_1 = 1, Z_2 = 0) = \frac{1}{10}.\end{aligned}$$

The value of $\frac{9}{10}$ can be any arbitrary constant close to 1 and δ_d should decrease to 0 as $d \rightarrow \infty$.

We remark the following Corollary, which is an obvious result from the property of the tree distribution in (2).

Corollary 1. *Given a tree distribution $P(x)$ in (2) with tree structure $T_P = (\mathcal{V}, \mathcal{E}_P)$, for arbitrary node pair (a, b) , there is a unique path $W((a, b); \mathcal{E}_P) := \{W_0(= a), \dots, W_l(= b)\}$ between X_a and X_b , such that $(W_k, W_{k+1}) \in \mathcal{E}_P$ for $1 \leq k \leq l - 1$. Moreover, the joint distribution for the path $W((a, b); \mathcal{E}_P)$ is given by*

$$\begin{aligned}P(W_0 = w_0, \dots, W_k = w_k, \dots, W_l = w_l) \\ = P(W_0 = w_0) \prod_{k=0}^{l-1} P(W_{k+1} = w_{k+1} | W_k = w_k).\end{aligned}\tag{35}$$

From the Corollary 1, the mutual information among the node variables $X \cup Y \cup \{Z_0\}$ is determined by the length of the path, *i.e.*, the number of hops, between them. Since the tree has a diameter of 4, a length of the path between arbitrary nodes in $X \cup Y \cup \{Z_0\}$ is either 1, 2, 3, or 4 with corresponding mutual information of I_1, I_2, I_3 , or I_4 , respectively. For example, between two nodes X_i and X_k , there is a path (X_i, X_j, X_k) in tree $T_{\bar{P}}$. From the simple calculation, the joint distribution is

$$\begin{aligned}\bar{P}(X_i = 1, X_k = 1) &= \bar{P}(X_i = 1 | X_j = 0) \bar{P}(X_j = 0 | X_k = 1) \bar{P}(X_k = 1) \\ &\quad + \bar{P}(X_i = 1 | X_j = 1) \bar{P}(X_j = 1 | X_k = 1) \bar{P}(X_k = 1)\end{aligned}$$

$$= \frac{1}{2} \left(\left(\frac{1}{2} + \delta_d \right)^2 + \left(\frac{1}{2} - \delta_d \right)^2 \right) = \frac{1}{4} + \frac{1}{2} \cdot 2\delta_d^2.$$

Consequently, we can easily check that

$$I_k = \left(\frac{1}{2} + m_k \right) \ln(1 + 2m_k) + \left(\frac{1}{2} - m_k \right) \ln(1 - 2m_k),$$

where $m_k = 2^{k-1}\delta_d^k$ for $k = 1, 2, 3, 4$. By using the Taylor approximation for \ln function, we have as $\delta_d \rightarrow 0$,

$$I_k \cong 4m_k^2 \cong (2\delta_d)^{2k}.$$

Moreover, mutual information among the variables Z_i s are given by

$$I(Z_0, Z_1) = I(Z_1, Z_2) = \alpha_1 = 0.368, \quad I(Z_0, Z_2) = \alpha_2 = 0.237.$$

We also can get the exact mutual information value between the node variables in $X \cup Y \cup \{Z_0\}$ and Z_1 or Z_2 , however, it is obvious that it is less than I_1 , which is enough for our remaining proof.

Construction of the communication cost functions \bar{c}^γ . Before the construction of the cost functions $\{\bar{c}_{i,j}^\gamma\}_{(i,j) \in \mathcal{E}}$, we consider a supergraph $\mathcal{S} = (\mathcal{V}, \mathcal{E}_\mathcal{S})$ of the constructed tree $T_{\bar{P}}$. The supergraph \mathcal{S} has the same node set \mathcal{V} but super edge set $\mathcal{E}_\mathcal{S}$ where all subset nodes in Y are connected to the *exactly* 3 element nodes in X .

Now, we can classify the edges in the complete graph $\mathcal{G} = (\mathcal{V}, \mathcal{E})$ into the following 9 types according to its mutual information and communication cost values.

$$\begin{aligned} \text{T1} : (X_i, Y_j) \in \mathcal{E}_{\bar{P}}, \quad \text{T2} : (X_i, Y_j) \in \mathcal{E}_\mathcal{S} \setminus \mathcal{E}_{\bar{P}}, \quad \text{T3} : (X_i, Y_j) \in \mathcal{E} \setminus \mathcal{E}_\mathcal{S}, \\ \text{T4} : (Y_i, Y_j) \in \mathcal{E}, \quad \text{T5} : (Y_j, Z_0) \in \mathcal{E}, \quad \text{T6} : (X_i, Z_0) \in \mathcal{E}, \\ \text{T7} : (X_i, X_j) \in \mathcal{E}, \quad \text{T8} : (Z_0, Z_1), (Z_1, Z_2), \quad \text{T9} : \text{others}. \end{aligned}$$

The corresponding mutual information and cost function of each type of edges are presented in Table 1. The cost of edges in T8 and (Z_1, X_i) and (Z_1, Y_j) in T9 are set to be κ , and the cost of (Z_2, X_i) and (Z_2, Y_j) in T9 are set to be 2κ , where $I_1 < \kappa$ as $s \rightarrow \infty$. One can easily check that the constructed cost functions $\{\bar{c}_{i,j}^\gamma\}_{(i,j) \in \mathcal{E}}$ satisfy the triangle inequality.

Optimal spanning tree T^* . From the objective function in (??), our optimal spanning tree is a maximum weight spanning tree (MWST) where the weight of edge (i, j) is defined as $w_{i,j} = I(P_{i,j}) - D_{T^*} \cdot c_{i,j}^\gamma$. There are two main reasons that difficulty of this problem arise. First, the MWST with the weight $I(P_{i,j}) - 2 \cdot c_{i,j}^\gamma$ could be different from the MWST with the weight $I(P_{i,j}) - 6 \cdot c_{i,j}^\gamma$. Second, MWST with the weight from a specific diameter value has no guarantee that it has the certain diameter. For example, even though we get a MWST with the weight $I(P_{i,j}) - 2 \cdot c_{i,j}^\gamma$, we cannot assure its diameter is 2. To handle these issues, we will show that under the constructed scenario of \bar{P} and \bar{c}^γ in Table 1, the diameter of the optimal spanning tree is always 4. For simplicity, we denote by T^* by the optimal spanning tree under the \bar{P} and \bar{c}^γ ,

Table 1: Mutual information $I(\bar{P})$ and the communication cost $\bar{c}_{i,j}^\gamma$ for each type of eadges

Edge type	(Mutual information, Communication cost)
T1	(I_1, I_1)
T2	$(I_3, \frac{3}{4}I_1 + \frac{1}{4}I_3)$
T3	$(I_3, \frac{3}{4}I_1 + \frac{1}{4}I_2 + \frac{1}{4}I_3)$
T4	$(I_2, \frac{3}{4}I_1 + \frac{1}{4}I_2)$
T5	$(I_1, \frac{3}{2}I_1)$
T6	$(I_2, \frac{11}{8}I_1 + \frac{1}{4}I_2)$
T7	$(I_2, \frac{11}{8}I_1 + \frac{1}{4}I_2)$
T8	$(\alpha_1 = 0.368, \kappa)$
T9	(Less than I_1 except $\alpha_2 = I(Z_0, Z_2)$, κ or 2κ)

i.e., T^* is a maximum weight spanning tree with the weight $I(\bar{P}_{i,j}) - D_{T^*} \cdot \bar{c}_{i,j}^\gamma$, and moreover, it is attained when $D_{T^*} = 4$.

Reduction to the X3C Problem. With the supergraph \mathcal{S} , we can make an instance for **X3C** problem. The nodes X_1, \dots, X_{3s} and Y_1, \dots, Y_q correspond to the element nodes and subset nodes in **X3C** problem, respectively. The 3 element nodes connected to each subset node Y_j stand for the 3-element subsets of Y_j . It is clear that we have total $d = 3s + q + 3$ number of nodes. For simplicity, we denote by $T_k^* = (\mathcal{V}, \mathcal{E}_k^*)$ the optimal spanning tree with a fixed diameter k . That is, we re-express the objective function for a fixed $k = 2, \dots, d-1$,

$$\bar{\mathcal{O}}_k^\gamma(T) = \sum_{(i,j) \in \mathcal{E}_T} I(\bar{P}_{i,j}) - k \cdot \sum_{(i,j) \in \mathcal{E}_T} \bar{c}_{i,j}^\gamma,$$

and thus $T_k^* = \arg \max_{T \in \mathcal{T}} \bar{\mathcal{O}}_k^\gamma(T)$. It is obvious that the optimal solution tree T^* is the best spanning tree among $\{T_k^*\}_{k=2, \dots, d-1}$. We now state our main result in following Lemma that if we find T^* , we can decide whether there is a solution for the **X3C** problem.

Lemma A.1. *Suppose that the mutual information $I(\bar{P})$ and cost functions \bar{c}^γ are defined as in Table 1. Let $\delta_d = \frac{\alpha_1 - \alpha_2}{\sqrt{4(3s+q)}}$ and $\kappa = \frac{9}{8}sI_1$. Then, there is a solution of the corresponding **X3C** problem if and only if the diameter of T^* is 4, i.e., $D_{T^*} = 4$, and*

$$\begin{aligned} \mathcal{O}^\gamma(T^*) &= \sum_{(i,j) \in \mathcal{E}_{T^*}} I(\bar{P}_{i,j}) - D_{T^*} \sum_{(i,j) \in \mathcal{E}_{T^*}} \bar{c}_{i,j}^\gamma \\ &= 2\alpha_1 - (11s + 3q)I_1 - 8\kappa. \end{aligned}$$

Proof. Suppose there is a solution of the **X3C** problem.

Find T_3^*, T_4^* and T_5^* . First, we decide T_3^*, T_4^* and T_5^* under the constructed joint distribution $\bar{P}(x)$ and communication costs \bar{c} . Under our scenario, from the fact that

Table 2: Edge weight $I(\bar{P}_{i,j}) - D_T \cdot \bar{c}_{i,j}^\gamma$ with different D_T

Edge type	Weight for $D_T = 3$	$D_T = 4$	$D_T = 5$
T1	$-2I_1$	$-3I_1$	$-4I_1$
T2	$-\frac{9}{4}I_1 + \frac{1}{4}I_3$	$-3I_1$	$-\frac{15}{4}I_1 - \frac{1}{4}I_3$
T3	$-\frac{15}{4}I_1 - \frac{3}{4}I_2 + \frac{1}{4}I_3$	$-5I_1 - I_2$	$-\frac{25}{4}I_1 - \frac{5}{4}I_2 - \frac{1}{4}I_3$
T4	$-\frac{9}{4}I_1 + \frac{1}{4}I_2$	$-3I_1$	$-\frac{15}{4}I_1 - \frac{1}{4}I_2$
T5	$-\frac{7}{2}I_1$	$-5I_1$	$-\frac{13}{2}I_1$
T6	$-\frac{33}{8}I_1 + \frac{1}{4}I_2$	$-\frac{11}{2}I_1$	$-\frac{55}{8}I_1 - \frac{1}{4}I_2$
T7	$-\frac{33}{8}I_1 + \frac{1}{4}I_2$	$-\frac{11}{2}I_1$	$-\frac{55}{8}I_1 - \frac{1}{4}I_2$
T8	$\alpha_1 - 3\kappa$	$\alpha_1 - 4\kappa$	$\alpha_1 - 5\kappa$
T9	Less than $I_1 - 3\kappa$	$I_1 - 4\kappa$	$I_1 - 5\kappa$

$\delta_d = \frac{\alpha_1 - \alpha_2}{\sqrt{4(3s+q)}}$, $\kappa = \frac{9}{8}sI_1$ and $I_k \cong (2\delta_d)^{2k}$, we have following order of values, (for large d)

$$\alpha_1 > \alpha_2 > \kappa > I_1 > I_2 > I_3.$$

Then, it is obvious that these trees must include two specific edges in T8, i.e., (Z_0, Z_1) and (Z_1, Z_2) , since edges in T8 have the largest weight compared to all other edges.

We now decide the structure of $T_3^* = (\mathcal{V}, \mathcal{E}_3^*)$. From the weight values of each type of edges in Table 2, it is clear that the edge set \mathcal{E}_3^* would be given by:

$$\mathcal{E}_3^* = \text{T5} \cup \text{T6} \cup \text{T8},$$

then its objective value is

$$\begin{aligned} \mathcal{O}^\gamma(T_3^*) &= \text{T5} \times q + \text{T6} \times 3s + \text{T8} \times 2 \\ &= \left(-\frac{7}{2}I_1\right) \times q + \left(-\frac{33}{8}I_1 + \frac{1}{4}I_2\right) \times 3s + (\alpha_1 - 3\kappa) \times 2 \\ &= -\left(\frac{99}{8}s + \frac{7}{2}q\right)I_1 + \frac{3}{4}sI_2 + 2\alpha_1 - 6\kappa. \end{aligned}$$

For the structure of $T_5^* = (\mathcal{V}, \mathcal{E}_5^*)$, it should be constructed as follows. The element nodes prefer to be connected to a subset node as T2 as possible, then to be connected as T1. Among the subset nodes, there is a unique center subset node and all other subset nodes are connected to the center node by T4, where the center subset node is connected to Z_0 , i.e., T5. Finally, two edges in T8 are included the tree. Now, the lower bound of the objective value is given by

$$\begin{aligned} \mathcal{O}^\gamma(T_5^*) &= \text{T2} \times 3s + \text{T4} \times (q-1) + \text{T5} + \text{T8} \times 2 \\ &\geq -\left(\frac{45}{4}s + 3q + \frac{9}{4}\right)I_1 - \frac{9}{4}I_2 + 2\alpha_1 - 10\kappa. \end{aligned}$$

We also highlight that the MWST for the weights $I(\bar{P}_{i,j}) - 5\bar{c}_{i,j}^\gamma$ (i.e., without constraint on the diameter of the constructed tree) is constructed to have a diameter

5 reveals that $\mathcal{O}^\gamma(T_5^*) \geq \bar{\mathcal{O}}_5^\gamma(T_6^*) \geq \mathcal{O}^\gamma(T_6^*)$. In consequence, it does not suffice to consider $T_k^*, \forall k \geq 6$.

Finally, we obtain the structure of $T_4^* = (\mathcal{V}, \mathcal{E}_4^*)$. As mentioned, two edges of T8, (Z_0, Z_1) and (Z_1, Z_2) , are included in \mathcal{E}_4^* . As seen in Table 2, edges of T1, T2 and T4 have larger weight than others, we need to contain as many edges of T1, T2 and T4 as possible. Therefore, there are two candidates for T_4^* . The first candidate tree, denoted by $T_4^{*,1} = (\mathcal{V}, \mathcal{E}_4^{*,1})$, is the tree where exactly s number of subset nodes, denoted by Y' , are connected to Z_0 by T5 and each subset node in Y' is connected to exactly 3 element nodes in X by T1 or T2. To retain a diameter of 4, remaining $q - s$ number of subset nodes in $Y \setminus Y'$ are connected with each other by constructing edges in T4. The corresponding objective value is given by

$$\begin{aligned} \mathcal{O}^\gamma(T_4^{*,1}) &= (\text{T1 or T2}) \times 3s + \text{T4} \times (q - s) + \text{T5} \times s + \text{T8} \times 2 \\ &= -(11s + 3q)I_1 + 2\alpha_1 - 8\kappa. \end{aligned} \quad (36)$$

It is now clear that this optimal tree $T_4^{*,1}$ exists if and only if there is a solution of **X3C** problem. In particular, finding optimal tree $T_4^{*,1}$ with objective value of $-(11s + 3q)I_1 + 2\alpha_1 - 8\kappa$, sub-collection $Y' \subset Y$ forms an exact cover of all element nodes in X .

Second candidate tree, denoted by $T_4^{*,2} = (\mathcal{V}, \mathcal{E}_4^{*,2})$, is the tree where only one center subset node is connected to Z_1 by T9. Then, there exist $3s$ number of edges in T2 and $q - 1$ number of edges in T4. The lower bound of the objective value of this tree is given by

$$\begin{aligned} \mathcal{O}^\gamma(T_4^{*,2}) &\geq \text{T2} \times 3s + \text{T4} \times (q - 1) + \text{T9} + \text{T8} \times 2 \\ &\geq -(9s + 3q - 2)I_1 + 2\alpha_1 - 12\kappa. \end{aligned} \quad (37)$$

From (36) and (37), we can observe that for $\kappa = \frac{9}{8}sI_1$, the optimal solution is attained at $T_4^{*,1}$, i.e., $\mathcal{O}^\gamma(T_4^{*,1}) > \mathcal{O}^\gamma(T_4^{*,2})$. Therefore, when solving the problem **SYNC**(n) in (13) to prove optimality on an instance constructed scenario of \bar{P}, \bar{c} , the question of the **X3C** problem can now simply be answered, i.e., the problem **SYNC**(n) is polynomially reducible to **X3C** problem, which completes the proof of Lemma. \square

The proof of NP-hardness of **SYNC**(n) in (13) is a direct consequence of Lemma A.1. \square

A.2 Proof of Theorem 2

The proof of Theorem 2 is quite similar and straightforward to that in [27].

A.3 Proof of Theorem 3

Proof. (i) Crossover rate. We present our proof into following 4 steps. In **Step 1**, we prove the existence of the crossover rate $J_{e,e'}(T)$, and in **Step 2**, we show the

expression of $J_{e,e'}(T)$ in (31). We then prove the existence of the optimizer Q^* and show that $J_{e,e'}(T) > 0$ in **Step 3**.

Step 1. First, we recall the definition of the crossover rate:

$$\begin{aligned} J_{e,e'}(T) &= \lim_{n \rightarrow \infty} -\frac{1}{n} \log \mathbb{P}(C_{e,e'}(T)) \\ &= \lim_{n \rightarrow \infty} -\frac{1}{n} \log \mathbb{P} \left(\left\{ w_e^{\text{Sync}}(T, \hat{P}(\mathbf{x}^{1:n})) \leq w_{e'}^{\text{Sync}}(T, \hat{P}(\mathbf{x}^{1:n})) \right\} \right). \end{aligned}$$

First, if $|r(T, e) - r(T, e')| \geq |\mathcal{X}| \log |\mathcal{X}|$, the crossover event $C_{e,e'}(T)$ is obviously empty set, since $|\mathcal{X}| \log |\mathcal{X}|$ is the maximum of the mutual information $I_e(\hat{P})$, which results the crossover rate $J_{e,e'}(T) = \infty$.

Now, assuming that $|r(T, e) - r(T, e')| < |\mathcal{X}| \log |\mathcal{X}|$, to prove the existence of the limit, we define the set $\mathcal{R} \subset \mathcal{P}(\mathcal{X}^4)$ by

$$\mathcal{R} := \left\{ Q \in \mathcal{P}(\mathcal{X}^4) : w_e^{\text{Sync}}(T, Q) \leq w_{e'}^{\text{Sync}}(T, Q) \right\},$$

then, we can re-express the crossover rate as

$$J_{e,e'}(T) = \lim_{n \rightarrow \infty} -\frac{1}{n} \log \mathbb{P}(\hat{P}_{e,e'} \in \mathcal{R}).$$

If \mathcal{R} is closed and $\mathcal{R} = \text{cl}(\text{int}(\mathcal{R}))$, then following is a direct consequence of the Sanov's theorem [36],

$$J_{e,e'}(T) = \lim_{n \rightarrow \infty} -\frac{1}{n} \log \mathbb{P}(\hat{P}_{e,e'} \in \mathcal{R}) = \inf_Q \{D_{\text{KL}}(Q \parallel P_{e,e'}) : Q \in \mathcal{R}\}.$$

It suffices to show that \mathcal{R} is closed and $\mathcal{R} = \text{cl}(\text{int}(\mathcal{R}))$, to complete the proof of the existence of the limit. First, for a fixed tree T , we define a function $h(Q) := w_{e'}^{\text{Sync}}(T, Q) - w_e^{\text{Sync}}(T, Q)$, which is a continuous function because the mapping $Q \mapsto Q_e$ and $I(Q_e)$ are continuous for any edge e , and the term $r(T, e)$ is constant on a fixed e . Therefore, \mathcal{R} is a closed set because it is an inverse image of a closed set by continuous function $h(Q)$. Second, it is trivial that $\mathcal{R}' := \{Q \in \mathcal{P}(\mathcal{X}^4) : w_e^{\text{Sync}}(T, Q) < w_{e'}^{\text{Sync}}(T, Q)\}$ is a subset of $\text{int}(\mathcal{R})$ from the fact that $h(Q)$ is continuous. Now, we choose an arbitrary distribution $M \in \mathcal{R} \setminus \mathcal{R}'$, where we can regulate either $I_e(M)$ or $I_{e'}(M)$ very slightly while maintaining the mutual information of the other edge, i.e., $I_e(M') = I_e(M) - \delta$ and $I_{e'}(M') = I_{e'}(M) + \delta$ for sufficiently small positive number δ . This distribution M' is included in \mathcal{R}' , since it still satisfies $w_e^{\text{Sync}}(T, M') < w_{e'}^{\text{Sync}}(T, M')$. We can always specify $M' \in \mathcal{R}'$ which converges to M as $\delta \rightarrow 0$, which concludes that \mathcal{R} is the closure of \mathcal{R}' . Finally, from the Sanov's theorem, we have the following expression of the crossover rate:

$$J_{e,e'}(T) = \inf_{Q \in \mathcal{P}(\mathcal{X}^4)} \{D_{\text{KL}}(Q \parallel P_{e,e'}) : w_e^{\text{Sync}}(T, Q) \leq w_{e'}^{\text{Sync}}(T, Q)\}. \quad (38)$$

Step 2. In **Step 2**, we show that if the optimal solution of (38), denoted by Q^* , exists, then it is attained when $w_e^{\text{Sync}}(T, Q^*) = w_{e'}^{\text{Sync}}(T, Q^*)$. We prove this by contradiction.

Suppose there is an optimal distribution M^* which minimizes the $D_{\text{KL}}(M_{e,e'}^* \parallel P_{e,e'})$ and satisfies $W(M_{e'}^*) > W(M_e^*)$. For $\lambda \in [0, 1]$, consider $M_{e,e'}^\lambda := (1 - \lambda)M_{e,e'}^* + \lambda P_{e,e'}$. As λ increases from 0 to 1, $h(M_{e,e'}^\lambda)$ moves from $h(M_{e,e'}^*)$ to $h(P_{e,e'})$ where $h(P_{e,e'})$ must be smaller than 0. $h(M_{e,e'}^\lambda)$ is a continuous function with respect to λ . Thus, there must be $\lambda \in (0, 1)$ such that $h(M_{e,e'}^\lambda)$ equals to 0 and $M_{e,e'}^\lambda \in R \setminus R'$. We can use the convexity of the KL-divergence to prove the contradiction.

$$\begin{aligned} D_{\text{KL}}(M_{e,e'}^\lambda \parallel P_{e,e'}) &= D_{\text{KL}}((1 - \lambda)M_{e,e'}^* + \lambda \cdot P_{e,e'} \parallel P_{e,e'}) \\ &\leq (1 - \lambda)D_{\text{KL}}(M_{e,e'}^* \parallel P_{e,e'}) + \lambda \cdot D_{\text{KL}}(P_{e,e'} \parallel P_{e,e'}) \\ &\quad (\because \text{Convexity of the KL-divergence}) \\ &= (1 - \lambda)D_{\text{KL}}(M_{e,e'}^* \parallel P_{e,e'}) < D_{\text{KL}}(M_{e,e'}^* \parallel P_{e,e'}). \end{aligned} \quad (39)$$

Therefore, we can derive the contradiction of the assumption about the existence of $M_{e,e'}^\lambda$ which is an element of $R \setminus R'$ and has smaller KL-divergence than $M_{e,e'}^*$. The conclusion in **Step 2** is

$$\inf_{M \in R} D_{\text{KL}}(M_{e,e'} \parallel P_{e,e'}) = \inf_{M \in R \setminus R'} D_{\text{KL}}(M_{e,e'} \parallel P_{e,e'}). \quad (40)$$

Step 3. Continuing from **Step 2**, we should show the existence of the minimizer $Q_{e,e'}^*$. If we can prove the compactness of $R \setminus R'$, we can get the existence of the minimizer $Q_{e,e'}^*$ in $R \setminus R'$ from Weierstrass' extreme value theorem. Therefore, by combining the result of **Step 2** or the equation (40), we can derive the existence of the minimizer $M_{e,e'}^*$. To prove the compactness of the $R \setminus R'$, we exploit Heine-Borel theorem and show the $R \setminus R'$ is bounded and closed. The boundedness is obvious because $\mathcal{P}(\mathcal{X}^4) \subset [0, 1]^{|\mathcal{X}|^4}$. The closedness is also obvious from the fact that $R \setminus R' = h^{-1}(\{0\})$.

Finally, we need to prove $J_{e,e'}(T) > 0$. Use contradiction. Suppose $J_{e,e'}(T) = 0$. That means

$$\inf_{Q \in \mathcal{P}(\mathcal{X}^4)} \{D_{\text{KL}}(Q \parallel P_{e,e'}) : W(Q_e) = W(Q_{e'})\} = 0.$$

Also in step 3, we find the existence of the minimizer $Q_{e,e'}^*$. That means $D_{\text{KL}}(Q_{e,e'}^* \parallel P_{e,e'}) = 0$, so $Q_{e,e'}^* \equiv P_{e,e'}$ and $W(P_e) = W(P_{e'})$. $W(P_e) = W(P_{e'})$ is a contradiction from the assumption $W(P_e) > W(P_{e'})$.

Consequently, from **Step 1**, **Step 2** and **Step 3**, we complete the proof of Theorem 3 (i).

(ii) **Error exponent.** We first get

$$\mathcal{A}_n(\gamma) \subset \bigcup_{t=1}^{d-1} \bigcup_{e' \in \mathcal{E}_c(\mathbb{T}_t) \setminus \mathbf{e}_t} C_{\mathbf{e}_t, e'}(\mathbb{T}_t). \quad (41)$$

Then, we will prove that for each step t of algorithm LearnSync, the below is correct,

$$\mathbb{P}(C_{\mathbf{e}_t, e'}(\mathbb{T}_t)) \leq \binom{n-1 + |\mathcal{X}|^4}{|\mathcal{X}|^4 - 1} \exp(-n \cdot J_{\mathbf{e}_t, e'}(\mathbb{T}_t)). \quad (42)$$

We can get the result (32) from the equations (41) and (42).

We can regard $\mathcal{A}_n(\gamma)$ be a union of the events that the SYNC algorithm finds the wrong tree-structure rather than the true tree-structure T at the final step d under the n samples. To find the wrong tree by the SYNC algorithm, we must find wrong edge e' among $\mathcal{E}_c(T_t) \setminus e_t$ which is the set of the possible edges at some step t for $t = 1, \dots, d-1$. Therefore we can easily get the eq (41). Unfortunately, we can not tell this union of the events exactly equals to $\mathcal{A}_n(\gamma)$. This is because we can choose the edges in kinds of reverse order. For example, we may choose e_{t+1} at the step t and choose e_t at the step $t+1$. Although this translation does not affect after the step $t+2$ or the final step, it is regarded as an error and included in $C_{e_t, e_{t+1}}(T_t)$ and $C_{e_{t+1}, e_t}(T_t)$ which are calculated as an error event.

(iii) Error probability. We derive the (42) from the result of (finite domain) Sanov's theorem in [37]

$$\mathbb{P}(C_{e_t, e'}(T_t)) \leq |\mathcal{L}_n| \exp(-n \cdot J_{e_t, e'}(T_t)), \quad (43)$$

where $|\mathcal{L}_n|$ represents the number of the possible empirical distributions $\hat{P}_{e, e'} \in \mathcal{P}(\mathcal{X}^4)$ by n samples. In [37], they use $(n+1)^{|\mathcal{X}^4|}$ as upper bound of $|\mathcal{L}_n|$. Although this bound is enough to prove the asymptotic property of Sanov's theorem, it is still very loose bound. We find exact value as $|\mathcal{L}_n| = \binom{n-1+|\mathcal{X}^4|}{|\mathcal{X}^4|-1}$. Suppose that you order $|\mathcal{X}^4| - 1$ number of black balls and n number of white balls in a row. The white balls would be divided into $|\mathcal{X}^4|$ partitions by the black balls. Let $a_1, a_2, \dots, a_{|\mathcal{X}^4|}$ be the number of the white balls in the each partitions by the black balls. It is obvious that $\sum_{i=1}^{|\mathcal{X}^4|} a_i = n$ and we can regard $(\frac{1}{n}a_1, \frac{1}{n}a_2, \dots, \frac{1}{n}a_{|\mathcal{X}^4|})$ as an empirical distribution by n samples on \mathcal{X}^4 . Therefore, the number of the combinations for the black balls and the white balls $\binom{n-1+|\mathcal{X}^4|}{|\mathcal{X}^4|-1}$ equals to $|\mathcal{L}_n|$. By substituting $|\mathcal{L}_n|$ into the eq (43), we get

$$\begin{aligned} \mathbb{P}(C_{e_t, e'}(T_t)) &\leq \binom{n-1+|\mathcal{X}^4|}{|\mathcal{X}^4|-1} \exp(-n \cdot J_{e_t, e'}(T_t)) \\ &\leq \binom{n-1+|\mathcal{X}^4|}{|\mathcal{X}^4|-1} \exp(-n \cdot K(\gamma)). \end{aligned} \quad (44)$$

From the fact that, we need to choose an edge among the edges between t nodes in T_t and $d-t$ nodes. At the step t under T_t , we have $t(d-t)$ candidates of edges in $\mathcal{E}_c(T_t)$. We finally get

$$\begin{aligned} \mathbb{P}(\mathcal{A}_n(\gamma)) &\leq \sum_{t=1}^{d-1} \sum_{e' \in \mathcal{E}_c(T_t) \setminus e_t} \mathbb{P}(C_{e_t, e'}(T_t)) \\ &\leq \left(\sum_{t=1}^{d-1} t(d-t) \right) \binom{n-1+|\mathcal{X}^4|}{|\mathcal{X}^4|-1} \exp(-nK(\gamma)) \\ &= \frac{(d-1)d(d+1)}{6} \binom{n-1+|\mathcal{X}^4|}{|\mathcal{X}^4|-1} \exp(-nK(\gamma)). \end{aligned} \quad (45)$$

The lower bound for the error exponent rate for $\mathbb{P}(\mathcal{A}_n(\gamma))$ can be derived as

$$\liminf_{n \rightarrow \infty} -\frac{1}{n} \log \mathbb{P}(\mathcal{A}_n(\gamma)) \geq K(\gamma).$$

We highlight that as $n \rightarrow \infty$, the resulting tree structure learned by SYNC algorithm equals to the *sub-optimal* cost efficient tree $\tilde{P}^\gamma(x)$ with respect to $\tilde{T}(\gamma) = (\mathcal{V}, \tilde{\mathcal{E}}(\gamma))$, with probability 1.

□